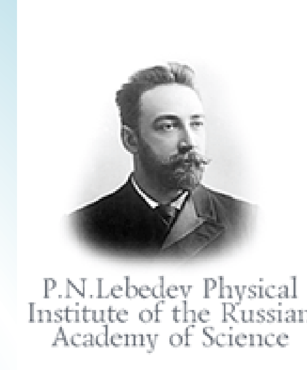

Стохастический нагрев электронов в микро-структурированных мишенях, облучаемых интенсивным лазерным излучением

Докладчик Бочкарев Сергей

ФИАН 04.02.2021

Межинститутском онлайн-семинар «Новые методы ускорения частиц и экстремальные состояния материи» **04/02/2020**

Объемно нагреваемые микро-структурированные мишени

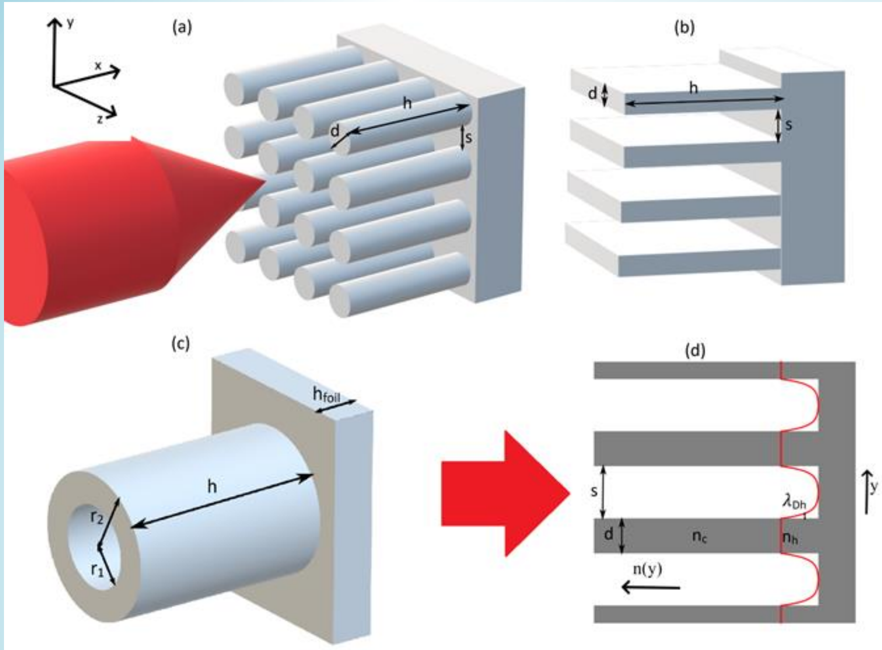

Прозрачность

Высокая средняя плотность

Эффективные объемный нагрев (почти полное поглощение лазерной энергии)

Применения

- горячие электроны, рентген, ускоренные ионы, позитроны, ТГц, возможность использования компактных лазеров с энергией ~20-50мДж, с частотой повторения 0.1-1кГц
- ядерные реакции «на столе» , high energy density research, пинчи

Применение микро-волосковой мишени для генерации нейтронов

A. Curtis et al., Nature Comm. **9** 1177 (2018)

Laser: 1.6 J, 60 fs , λ = 400 nm, $I_L \leq 8 \times 10^{19}$ Wcm^{-2}, spot 2.6 **μm diameter**

400 nm diameter, 5 μm long, CD_2 nanowires

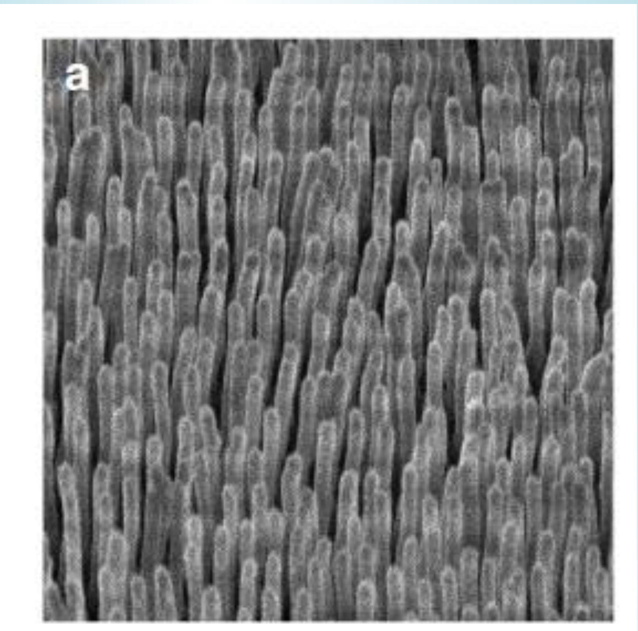

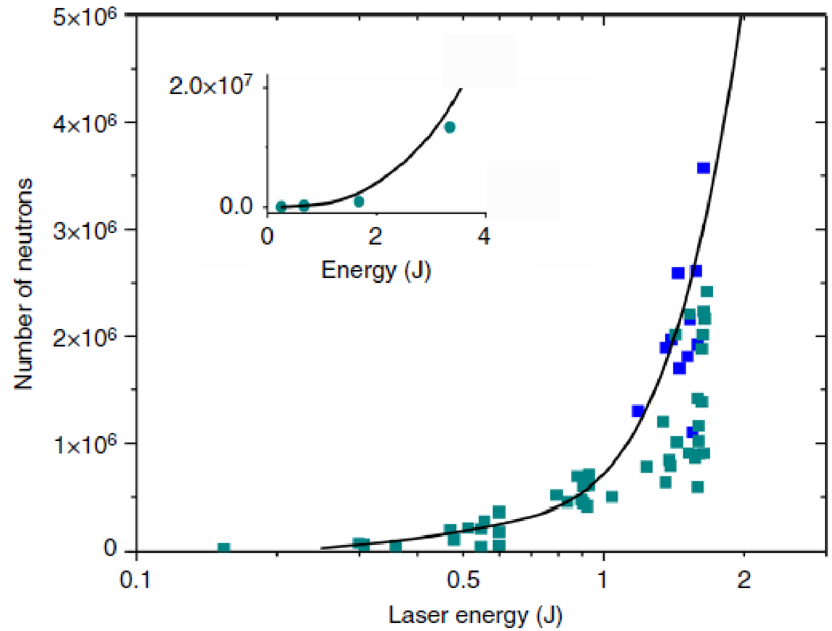

Fig. 5 Neutron yield as a function of laser pulse energy on target. The dark blue squares are shots corresponding to a target with 200 nm diameter wires. All the other shots (light blue squares) are for targets consisting of 400 nm diameter wire arrays. Each point resulted from the average of four scintillator/PMT time of flight detector signals. The line shows the simulated energy dependence of the neutron yield calculated using deuteron energy distributions computed by the PIC model and nuclear kinetics. The inset extends the simulation to 3.5 J, where the green circles are computed values of the neutron yield

Max yield $2 \cdot 10^6$ neutrons/J,
Yield per one deuteron ≈10^{-6}

Laser Fabrication of Nano Sheet (Wire) Arrays

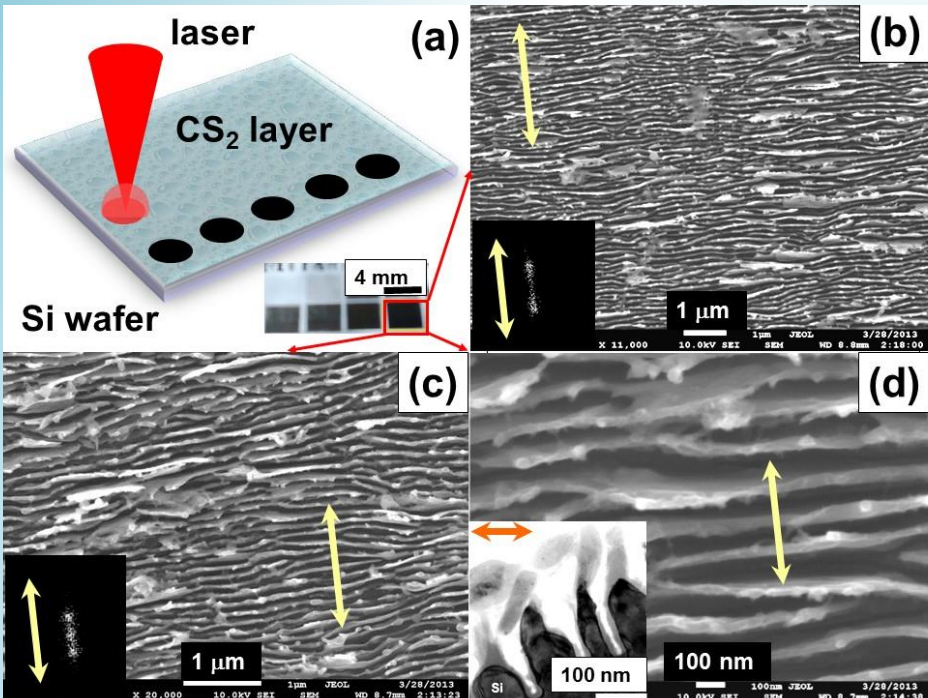

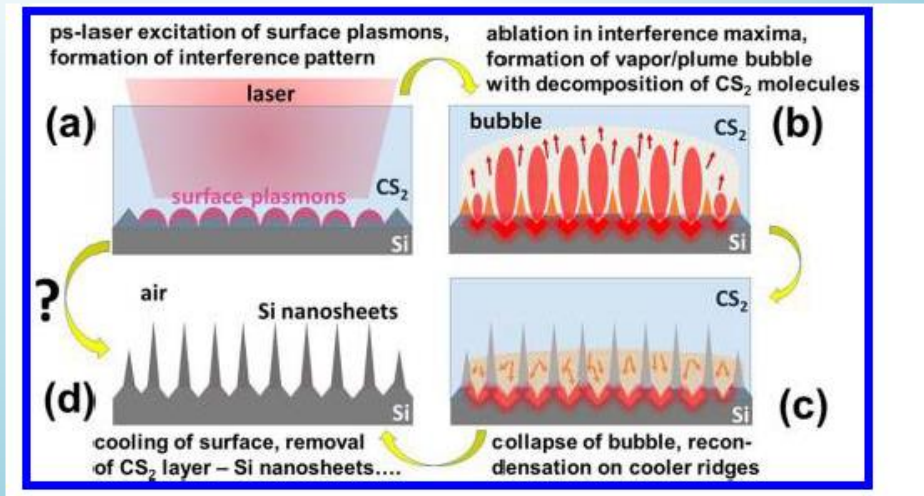

Nanoplasmonic Ablative Self-Organization

S.I. Kudryashov et al.,
ACS Appl. Nano Mater. 2461 (2018).

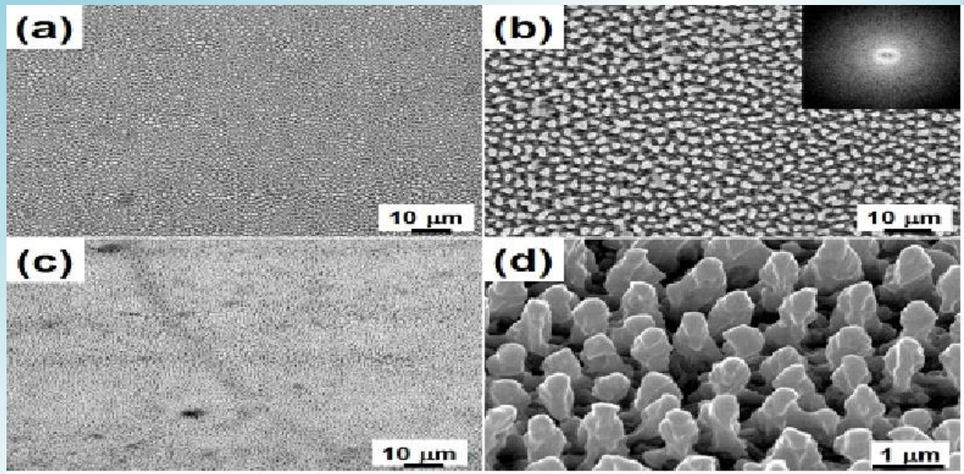

A.A. Ionin et al., Hydrodynamic instability and self-organization of a submicron relief on metal surfaces upon femtosecond laser exposure in liquids JETP Letters, 106 (2017)

Эксперименты по нагреву микроструктур

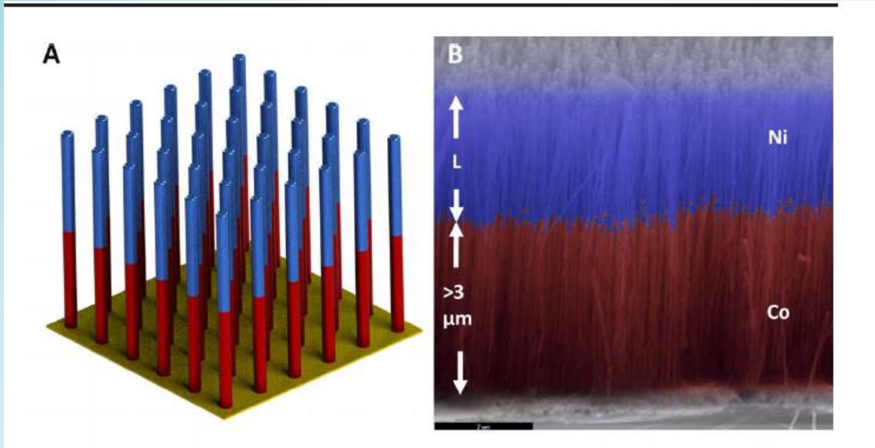

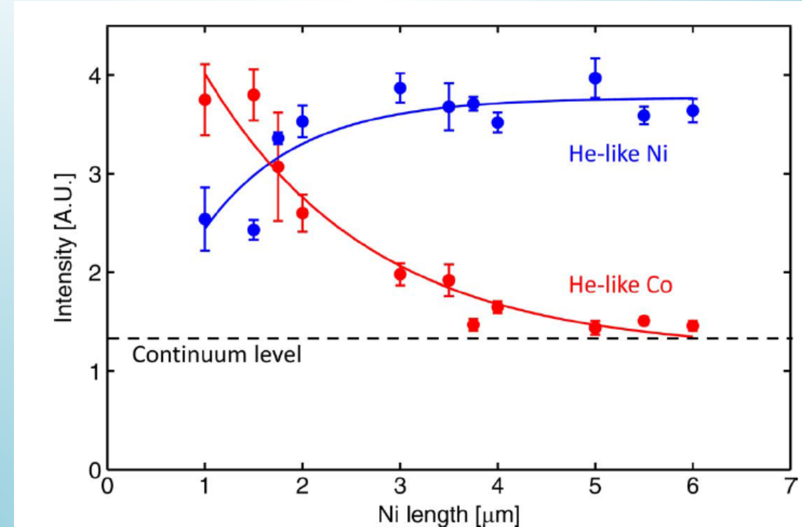

Fig. 3. Measured intensities of the He-like Co and Ni lines as a function of the length of the top Ni nanowire segment. The target and laser parameters are the same as those in Fig. 2.

Моделирование: давление ≈7 Гбар, термолизованная температура электронов ≈17 кэВ

Лазер: 0.6 Дж, 55 фс , λ = 400 nm (2ω), $I_L = 4 \times 10^{19}$ Wcm^{-2}, диаметр пятна 5 мкм, контраст >10^{12},

мишень из никеля, нанонити (55 нм диаметр), средняя плотность 13% твердотельной

Citation: C. Bargsten, R. Hollinger, M. G. Capeluto, V. Kaymak, A. Pukhov, S. Wang, A. Rockwood, Y. Wang, D. Keiss, R. Tommasini, R. London, J. Park, M. Busquet, M. Klapisch, V. N. Shlyaptsev, J. J. Rocca, Energy penetration into arrays of aligned nanowires irradiated with relativistic intensities: Scaling to terabar pressures. *Sci. Adv.* **3**, e1601558 (2017).

PIC моделирование нагрева мишени

Setup	τ_L(fs)	I_L(10^{18} W/cm^2)	focal spot (λ_L)	a_0	T_h^{PM}(keV)	ε_h^{EM}(keV)
I	30	1	4	0.85	85	185
II	60	2	2	1.2	160	370

$$T_h^{PM} = m_e c^2 \left(\sqrt{1+a_0^2/2}-1\right)$$

$$\varepsilon_h^{EM} = m_e c^2 a_0^2 / 2$$

Mandor code : 3D3V PIC parallel simulations,8 particles per cell, immobile ions

Box size: 7 λ_L x10 λ_L x10 λ_L,0.005 λ_L, x 0.02 λ_L, x 0.02 λ_L,

Linearly polarized laser pulse

Проникновение ЭМ поля в мишень

PIC, $I=2\cdot10^{18}$ W/cm², $D=2\,\lambda_L$, $\tau=60$ fs, $\lambda_L=1$ μm

h=1.5-7 λ_L

d=0.4λ_L

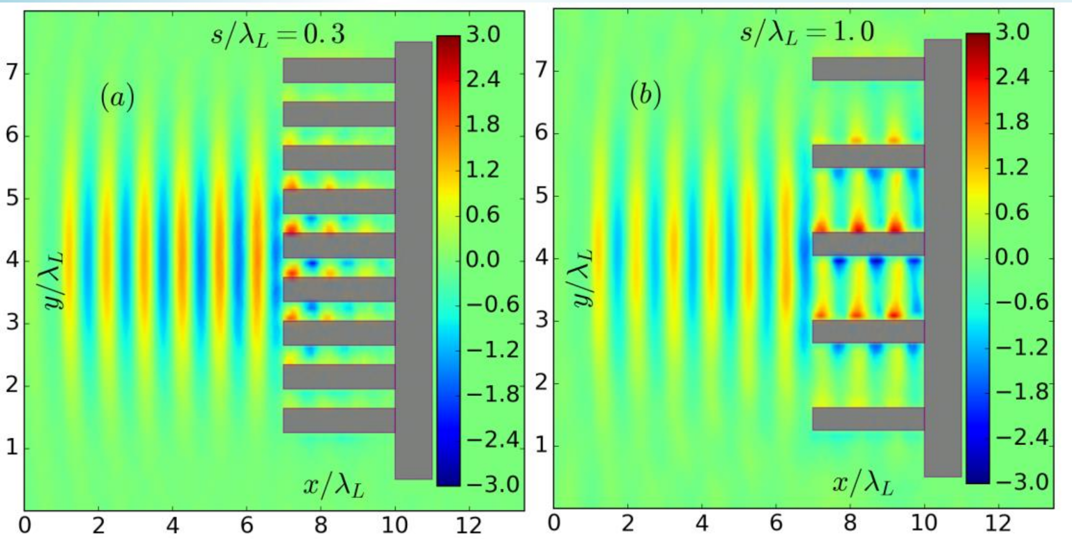

Amplitude of electric field

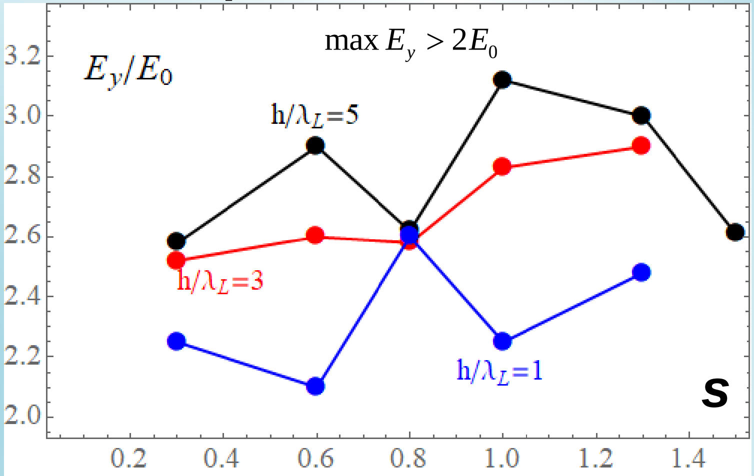

Maxwell solver, FIT

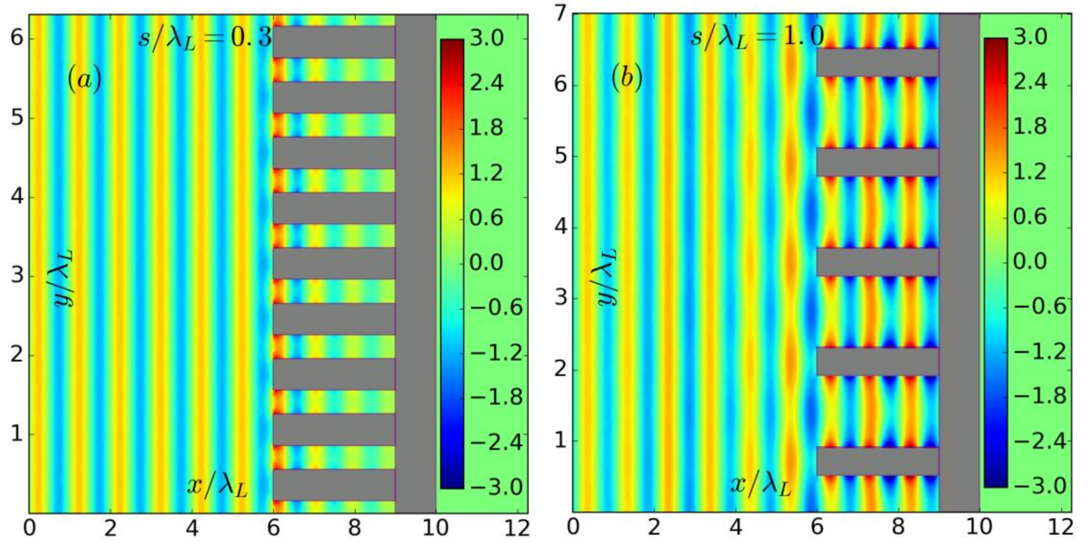

Penetration depth, PIC

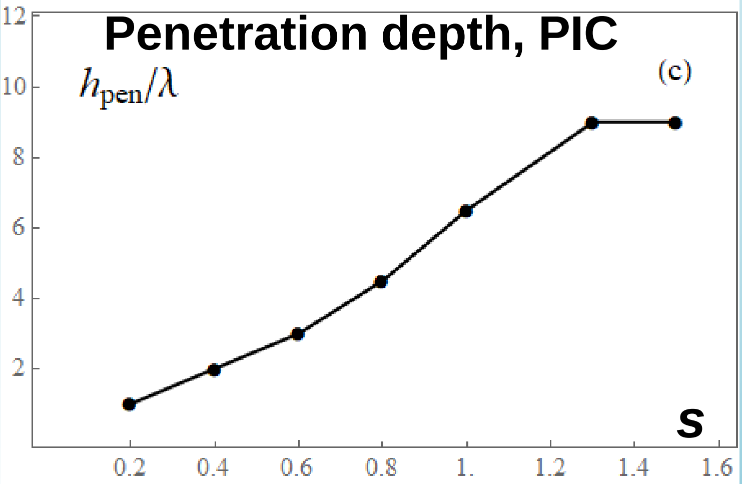

Оптимизация выхода горячих электронов

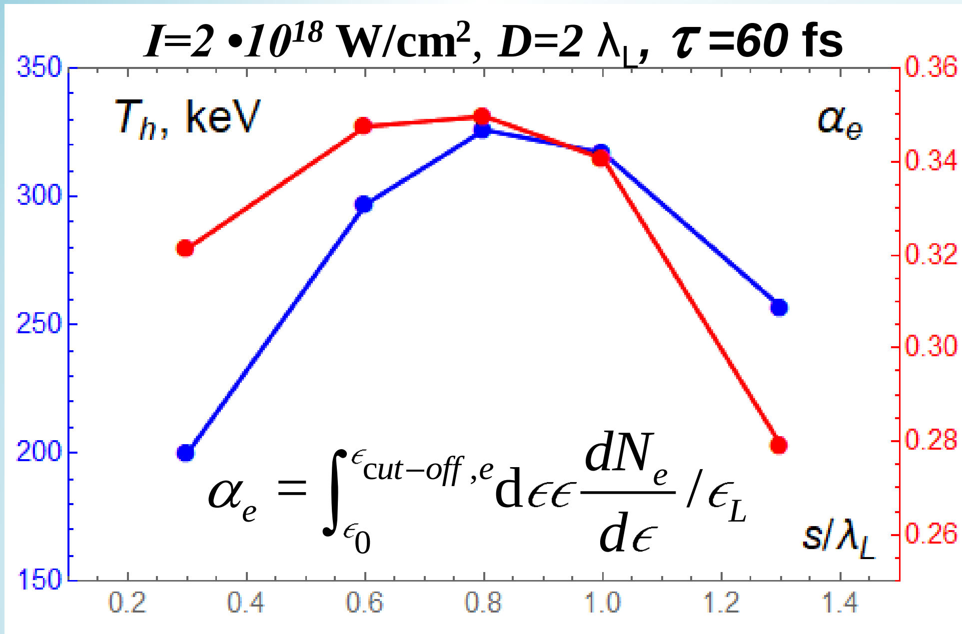

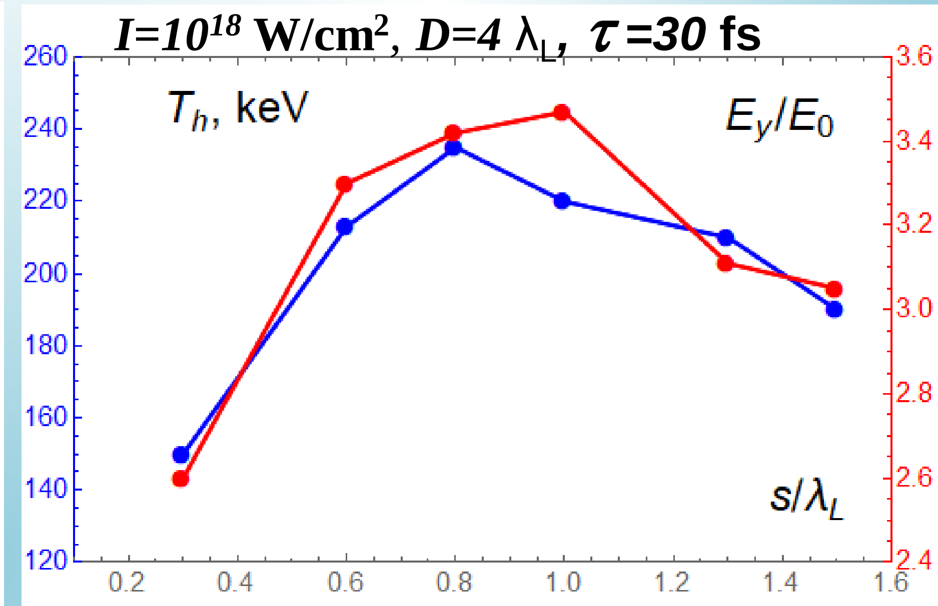

$$\epsilon_h^{\mathrm{EM}} = m_e c^2 (\gamma_{max} - 1) = m_e c^2 a_0^2/2,$$

$$T_h^{\mathrm{PM}} = \left((1 + a_0^2/2)^{1/2} - 1 \right) m_e c^2 \ , \quad a_0 \approx 1 \Rightarrow \epsilon_h^{\mathrm{EM}} \approx T_h^{\mathrm{EM}}$$

Acceleration beyond the ponderomotive limit !!!

$$\epsilon_{cut-off,e} \gg \epsilon_h^{EM} \approx 3\mathrm{MeV},$$

$$T_h > T_h^{\mathrm{EM}}$$

Оптимизация : температура горячих электронов

$I=2 \cdot 10^{18}$ W/cm^2, $D=2\,\lambda_L$ (FWHM), $\tau=60$ fs, $d=0.4\,\lambda_L$

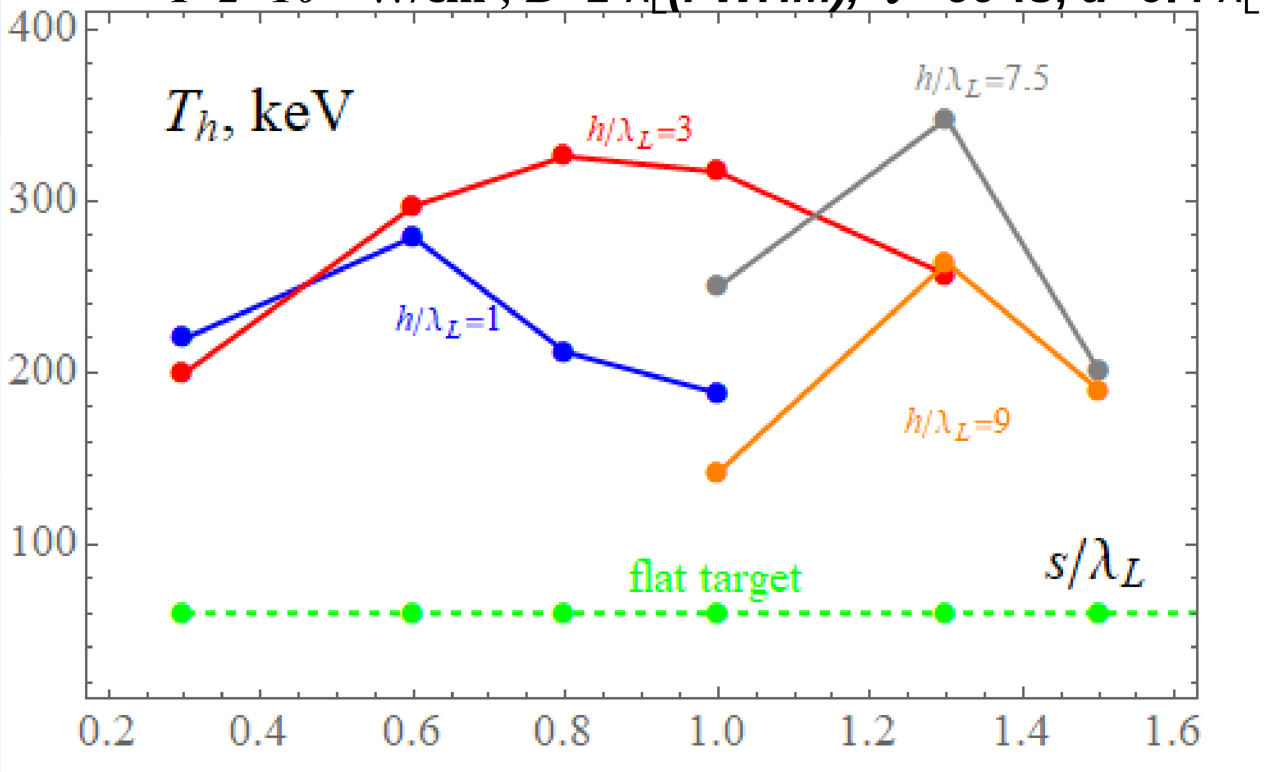

Absorption $\gtrsim$ 60%

flat surface ≈10%
$T_h \approx 50$ keV
($a_0 \approx 1.2$)

High average density

presence of wave reflected favors stochastic heating

Optimal conditions for electron heating

$$s \gtrsim 2r_E \sim d, \qquad h \sim h_{pen} \approx c\tau_L/2,$$

$$r_E = a_0 \lambda_L / 2\pi$$

Механизмы ускорения электронов в объемно-нагреваемых мишенях

JxB, Brunel, vacuum heating/direct laser acceleration (DLA)

stochastic electron acceleration/heating

spectra of electrons from micro-wire targets: two temperature

How to explain generation of super – ponderomotive particles?

Laser pulse field + arbitrary additional field (e.m. field, electrostatic field, Coulomb, magnetic field)

Динамика тестовых частиц в сложных полях

- 3D Test particle simulation

$$\frac{d}{dt}\vec{p} = -e\vec{E} - \frac{\vec{v}}{c}\times\vec{B}, \quad \frac{d}{dt}\vec{r} = \frac{\vec{p}}{m_e\gamma},$$

$$\vec{E} = \vec{E}_i + \vec{E}_r + \vec{E}_C$$

$$\vec{B} = \vec{B}_i + \vec{B}_r + \vec{B}_S$$

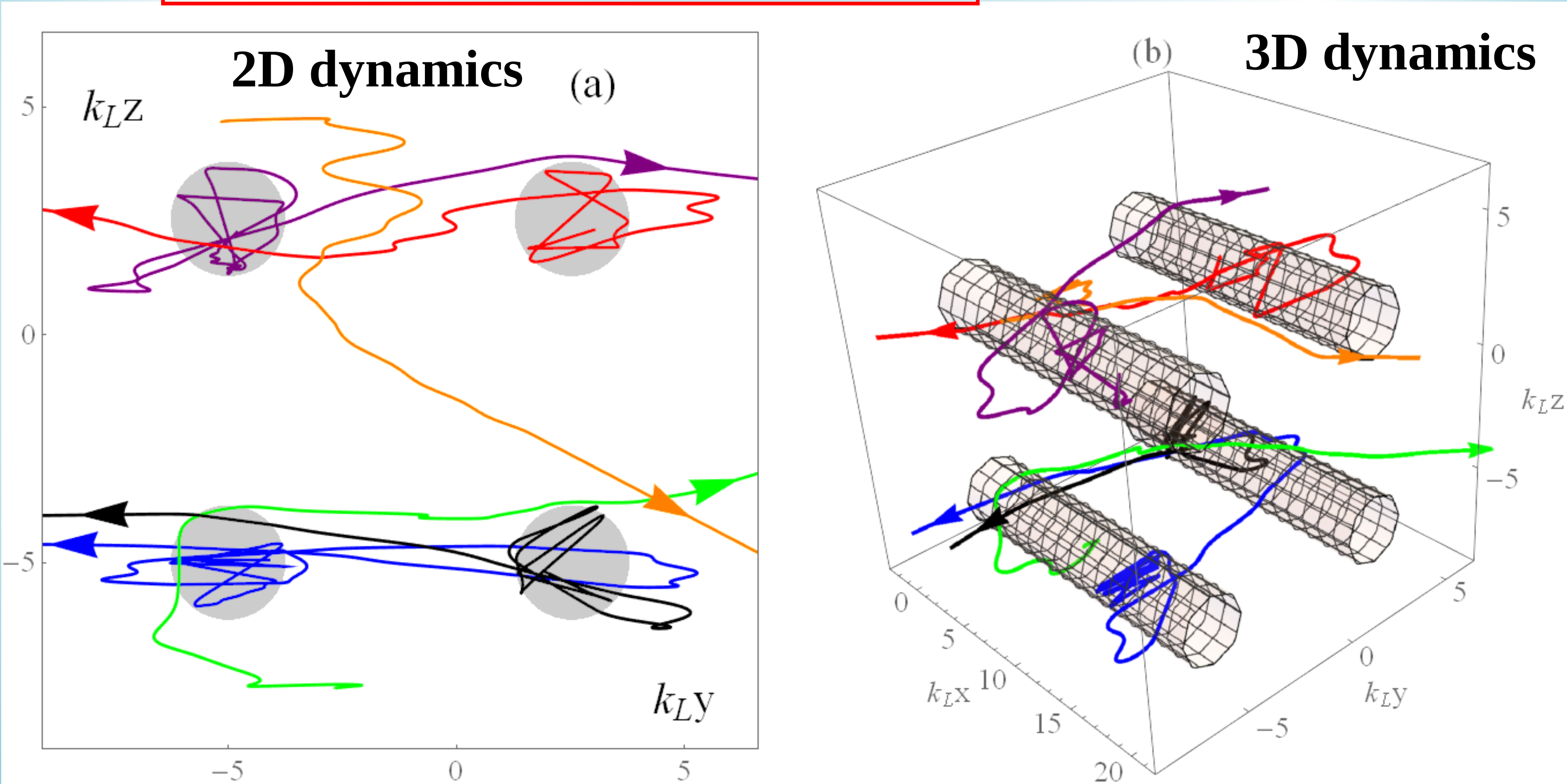

Описание квазистатических поле в микро структурах

$$E_y^i = E_0 f(r)\cos(\phi_-),\quad E_y^r = \hat{r}E_0 f(r)\cos(\phi_+ + \pi),\quad B_z^i = E_0 f(r)\cos(\phi_-),\quad B_z^r = \hat{r}E_0 f(r)\cos(\phi_+),$$

$$\phi_\pm = \omega_L t \pm k_L x + \phi_0,\ f(r) = \sum_{n=1}^{N_{str}} \exp\left(-\frac{(d/2 - |\vec{R}_n|)}{l_s}\right).$$

$$\vec{\mathbf{E}}^C(\vec{\mathbf{r}}) = E_{Q0}\frac{m_e c\omega_L}{e}\sum_{n=1}^{N_{str}}\begin{cases} 0, \\ \left(1 - \frac{d}{2l_s} + \frac{|\vec{\mathbf{R}}_n|}{l_s}\right)\frac{\vec{\mathbf{R}}_n}{|\vec{\mathbf{R}}_n|}, \\ \frac{C_Q\vec{\mathbf{R}}_n}{|\vec{\mathbf{R}}_n|^2}\exp\left(\frac{-|\vec{\mathbf{R}}_n|}{r_d}\right), \end{cases}$$

$$\vec{\mathbf{R}}_n = \vec{\mathbf{r}}_\perp - \vec{\mathbf{r}}_n,\quad C_Q = \frac{d}{2}\exp\left(\frac{d}{2r_d}\right),$$

$$\hat{r} \approx 0.7$$

$$E_{Q0}/E_0 \approx 0.7$$

$$B_{\phi 0}/E_0 \approx 0.6$$

$$j_\parallel(r = |\vec{\mathbf{R}}_n|) = -ecn_{\mathbf{cr}}B_{\phi 0}\begin{cases} 0, & r \le d/2 - l_s \\ C_{j1}(r - d/2 + l_s)(r - d/2), & d/2 - l_s < r \le d/2 \\ C_{j2}\exp\left(-\frac{r}{r_{\mathbf{E}}}\right)(r - d/2), & r > d/2. \end{cases}$$

$$B_\phi^0(r_\perp) = \frac{4\pi}{cr_\perp}\int_0^{r_\perp} j_\parallel(r)rdr.$$

Метод показателей Ляпунова

- **Definition**

$$\lambda_{\max} = \lim_{t\to\infty} \lim_{d(0)\to 0} \frac{1}{t} \ln \frac{d(\vec{x}_0, t)}{d(\vec{x}_0, 0)}, \qquad d = |\vec{X}(\vec{x}_0, t) - \vec{X}(\vec{x}_0 + \delta\vec{x}_0, t)|.$$

$$d \approx \exp(\lambda_{\max} t)$$

- **Method for calculation of the largest Lyapunov exponent**

$$\lambda_{\max,n} \approx \frac{1}{\Delta t} \sum_n \ln \frac{d_n}{d_0}, \qquad d_n = |\vec{y} - \vec{x}|_n,$$

$$\lambda_{\max} = \lim_{n\to\infty} \lambda_{\max,n}$$

here d_n - distance at time $t = t_n$

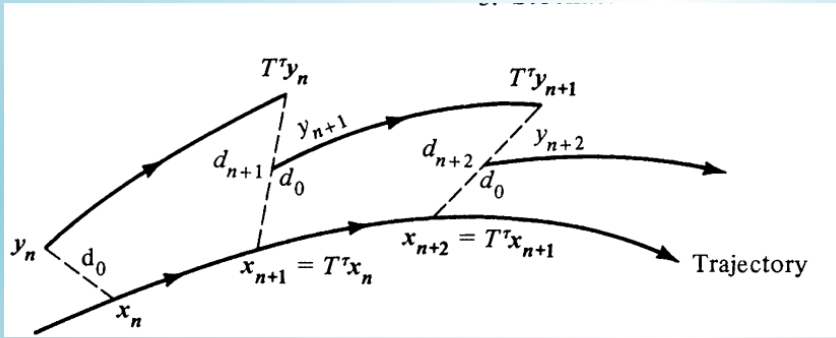

renormalization

$$\vec{r}_i \leftarrow \vec{R}_i + \frac{\vec{\rho}_i}{\alpha_i} \qquad \alpha_1 \equiv \frac{d(t_1)}{d(t_0)}$$

$$d(t) \geq D \qquad \vec{\rho} \equiv \vec{r} - \vec{R}.$$

Criteria of stochastic motion:

$$\lambda_{\max} > 0$$

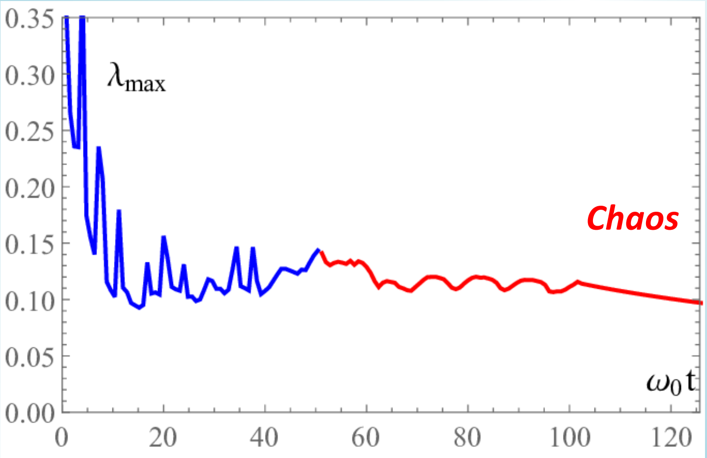

Анализ стохастического нагрева

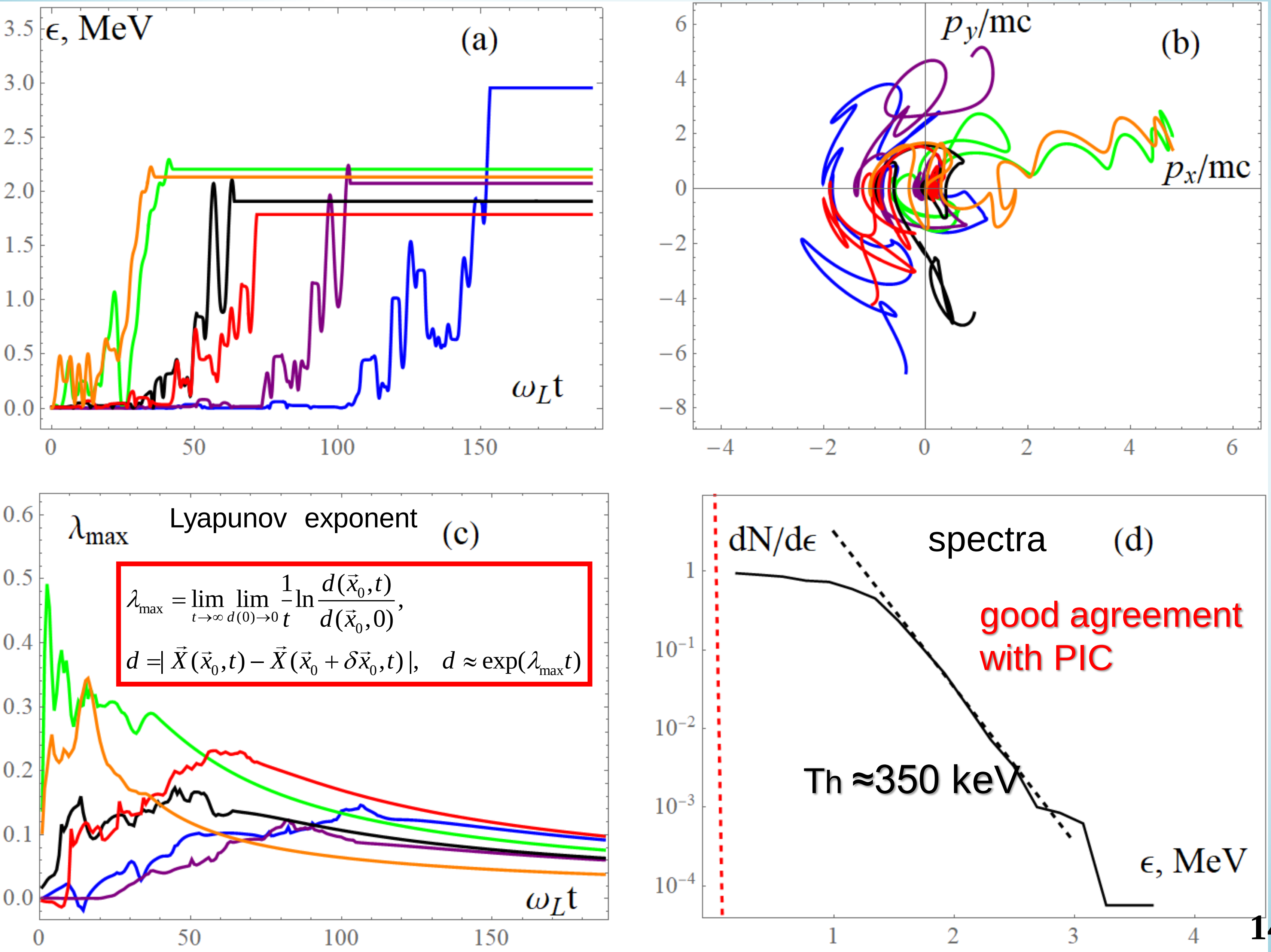

Угловое распределение ускоренных электронов

Angular distribution inside heated domain

Angular distribution of electrons leaving microstructures and entering substrate targets

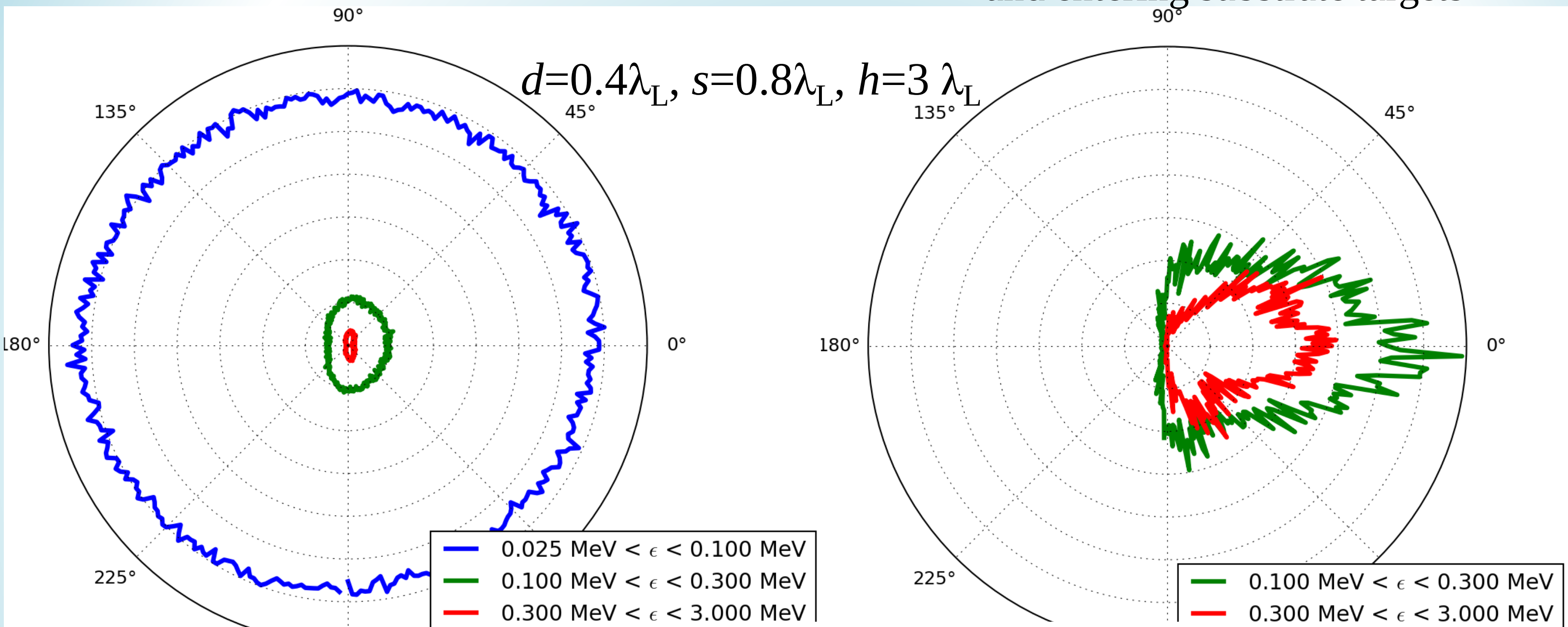

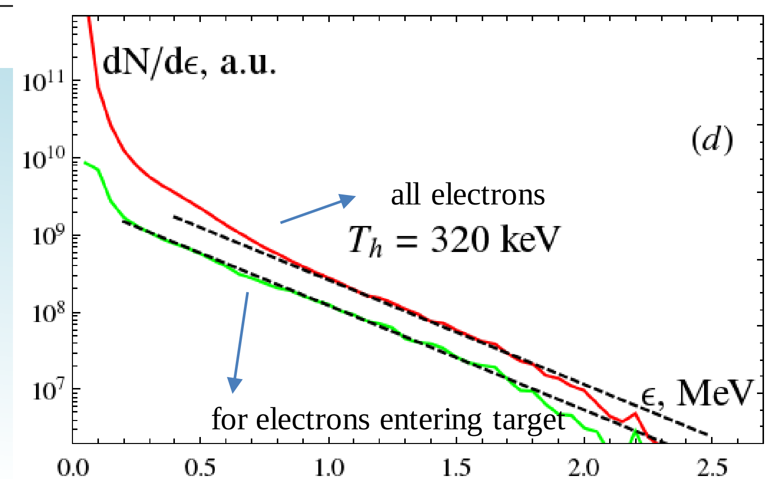

Conversion (energy > 100 keV) reaches ~ 10%.
MA beam current of hot electrons is formed,
return current heats target to the temperature of
~ 5 eV in the volume of 30 × 30 × 10 μm^3

3D моделирование : разлет плазмы

deuterated titanium wires 40% of deuterium 20% D and 20% T.

$d = 0.4\lambda_L, \quad h = 1.5\lambda_L$

$d = 0.3\lambda_L, \quad h = 1.5\lambda_L$

$t = 0$

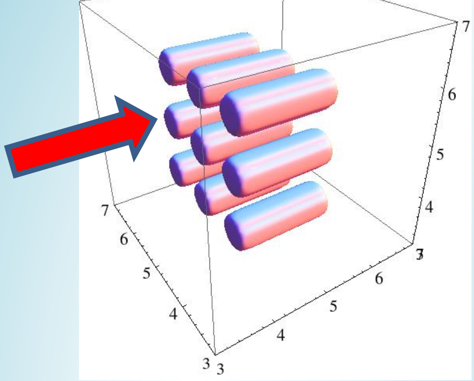

$t = 200\,fs$

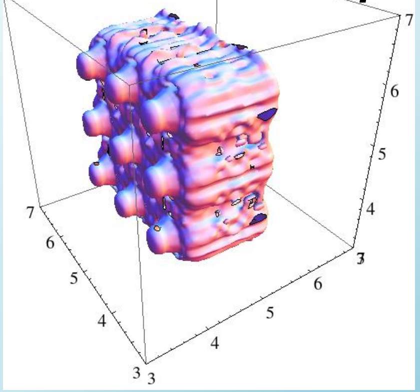

$t = 0$

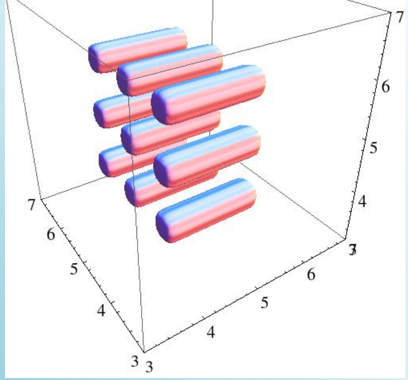

$t = 200\,fs$

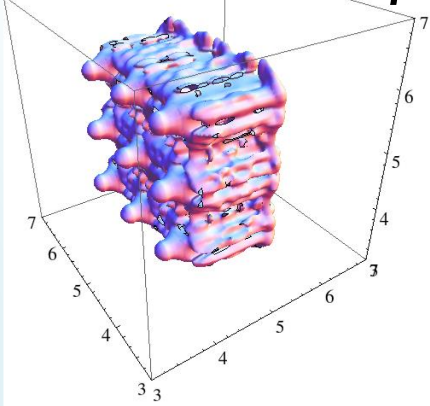

Ion distribution d^2N/dv_xdv_y

$t = 35\,fs$

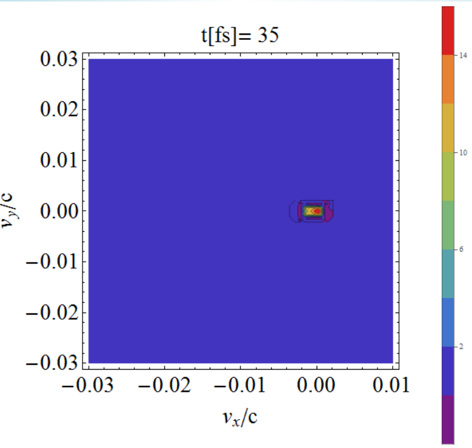

$t = 59\,fs$

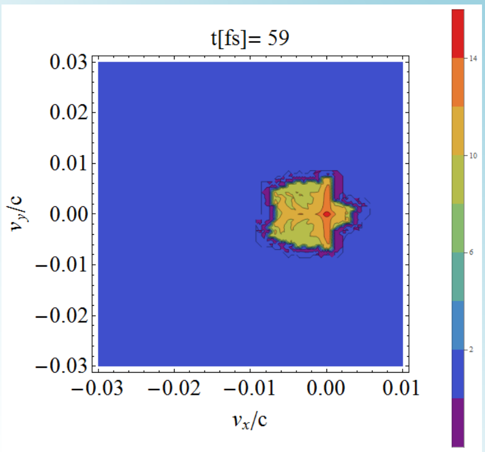

$t = 83\,fs$

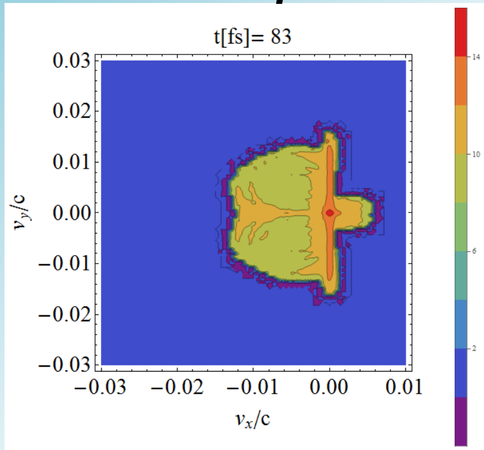

$t = 131\,fs$

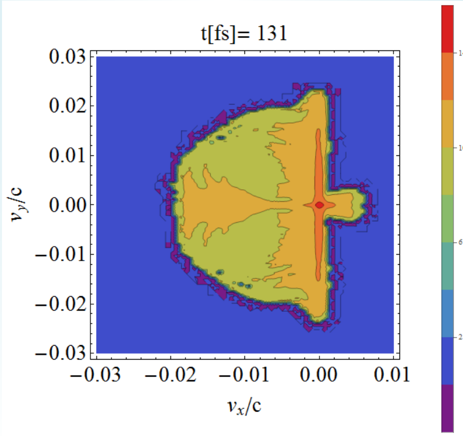

Plasma expands with velocity ≈2μm/ps, The cross section of DT reaction is large for deuterium energy of order of 100-500 keV.   Deuterons obtain such energy during laser heated cylinder expansion on characteristic scale equal to inter-wire spacing.

Спектры ускоренных дейтронов

We consider acceleration of deuterium and tritium ions implanted into pure metal sub-micro-sized surface structures

t=0 *d=0.4 λ$_L$, h = 2 λ$_L$* *t=200 fs*

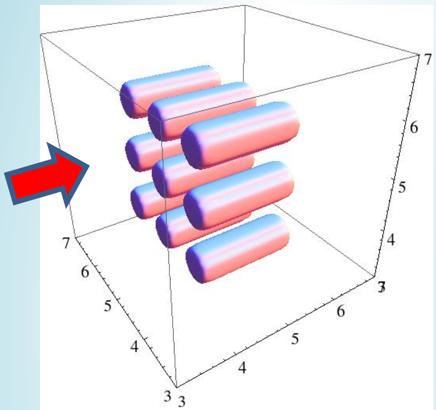

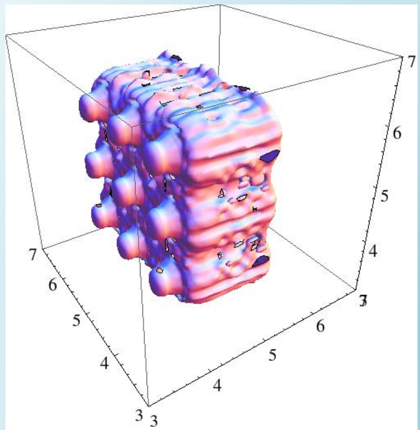

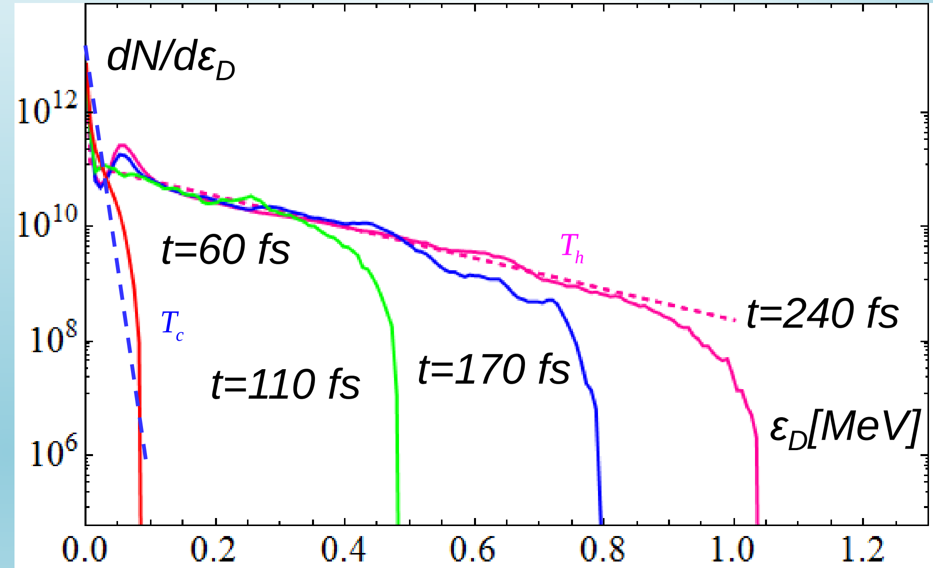

t=0 *d=0.3 λ$_L$, h = 2 λ$_L$* *t=200 fs*

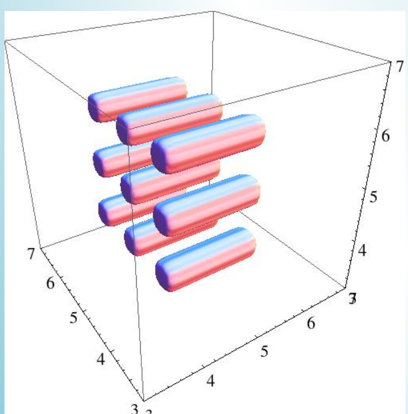

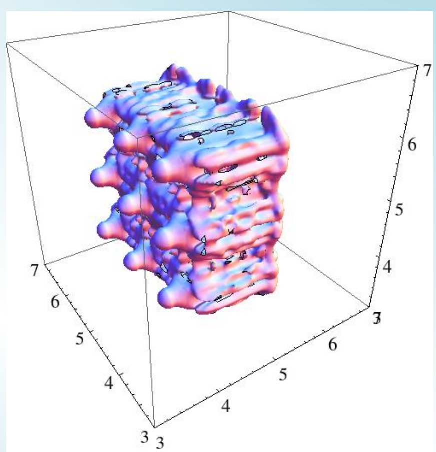

Conversion of energy into ions is about 6 (*d*=0.4 λ to 10 % (*d*=0.3 λ$_L$)

Approximation for spectrum

$$\frac{dN}{d\varepsilon_2} = \theta(\varepsilon_{ch} - \varepsilon_2) C n_{c0} \exp\left(\frac{-\varepsilon_2}{Z_2 T_c}\right) + \theta(\varepsilon_2 - \varepsilon_{ch}) C n_{h0} \exp\left(\frac{-\varepsilon_2}{Z_2 T_h}\right),$$

$$\varepsilon_{ch} = Z_2 T_c \ \ln(n_{c0}/n_{h0}),$$

V.F.Kovalev, S.G.Bochkarev and V.Yu.Bychenkov, *Quantum Electron.*, **47,** 1023 (2017).

Спектры ускоренных дейтронов от E_L

$D_L = 4\ \lambda_L$ (FMHW) duration – 30 fs

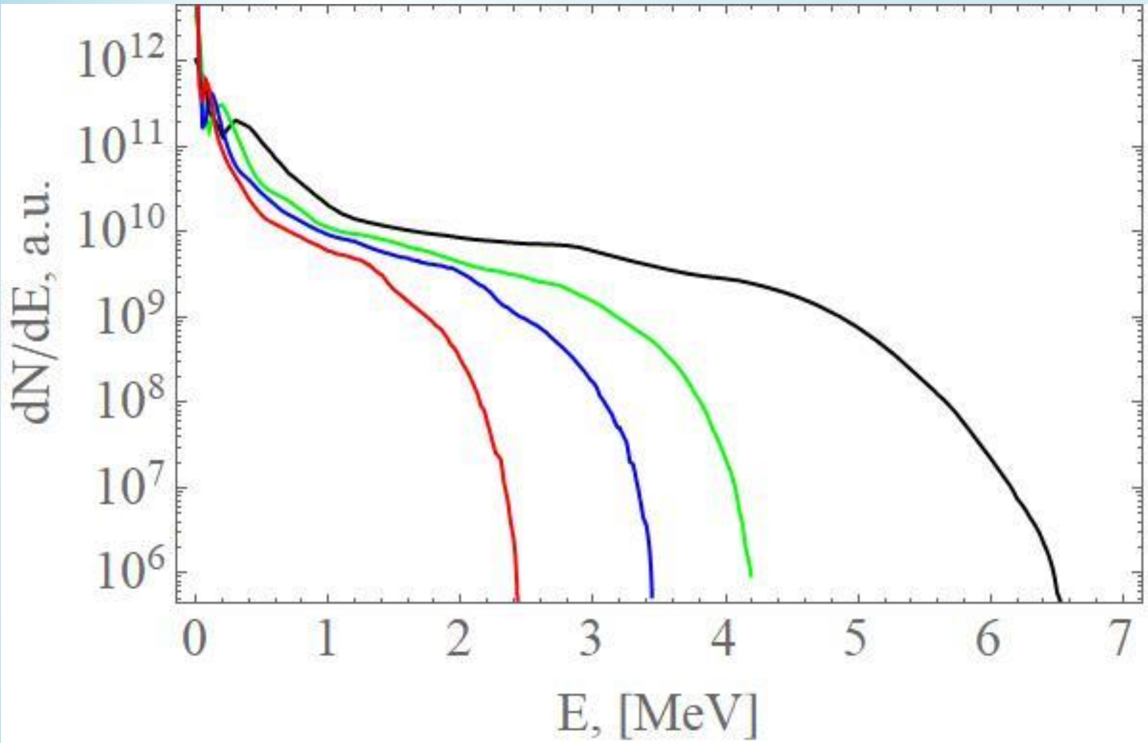

$$\varepsilon_{max} = 2T_h \left(\ln(\sqrt{2} t_{acc}\, \omega_{Dh}/\sqrt{\mathrm{e}})\right)^2$$

E_L=27 mJ - red, 54 mJ - blue, 108 mJ –green line и 270 mJ – black line

Multi sheet target

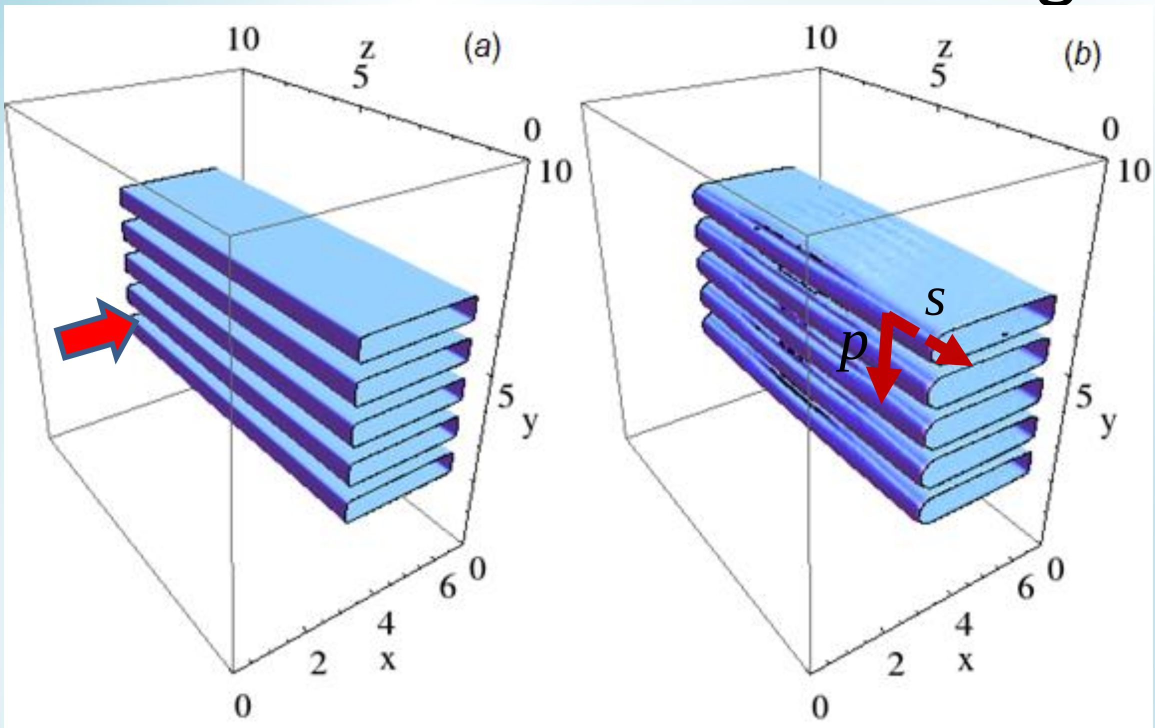

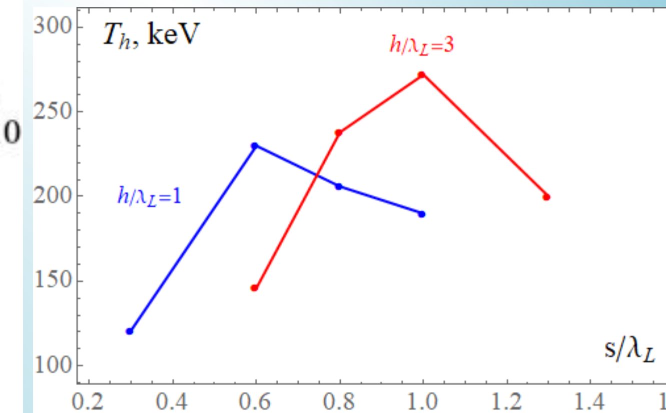

T_h ≈270 keV for **h = 3λ$_L$**, **s = 1λ$_L$**, **d= 0.4 λ$_L$** that is 20% less than for microwire target

$$T_h^{sheet} / T_h^{wire} \simeq \pi / (1 + s/d)$$

Difference between p and s polarization of laser pulse

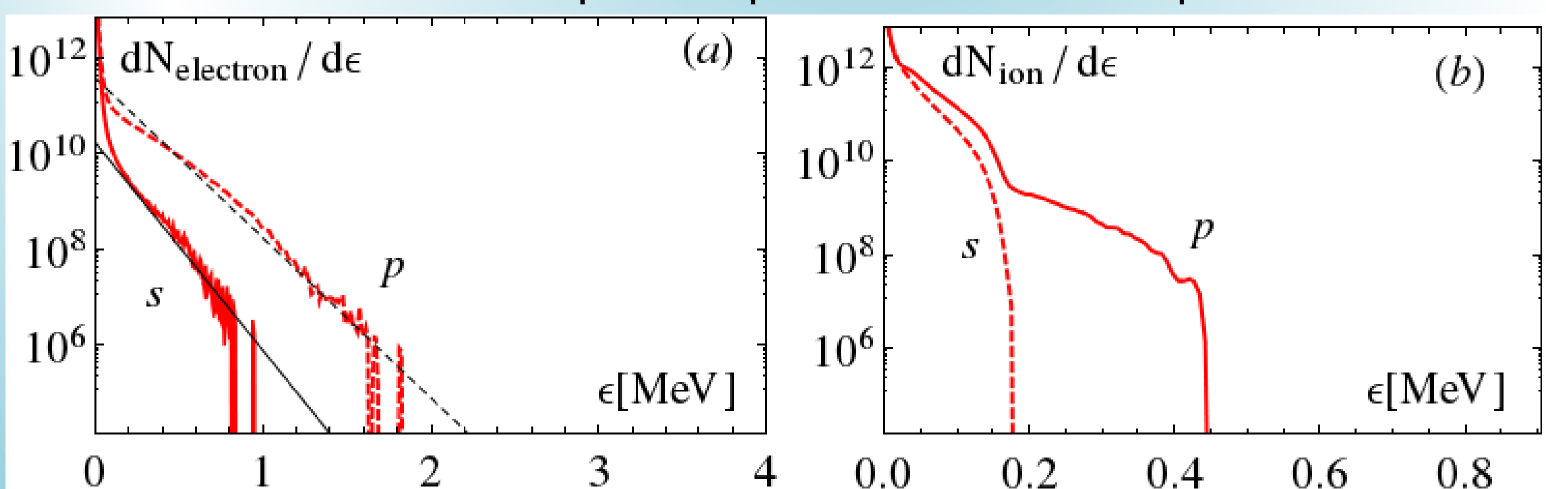

Расчет выхода DD и DT реакции

$$Y \equiv \frac{N}{N_{i0}} = \frac{1}{N_{i0}} \int_0^{\infty} d\epsilon \frac{dN_i}{d\epsilon} n_a \int_0^{\epsilon} d\epsilon' \sigma(\epsilon') \left| \frac{d\epsilon'}{dr} \right|^{-1}$$

The target consist from titanium and 40% of deuterium or 20% D and 20% T.

D+D→^{3}He + n +3.27 MeV, E_n= 2.45 MeV,

D+T→^{4}He + n +17.6 MeV, E_n= 14.1 MeV,

Cross-sections D(d,n)^{3}He, T(d,n)^{4}He from NRS book

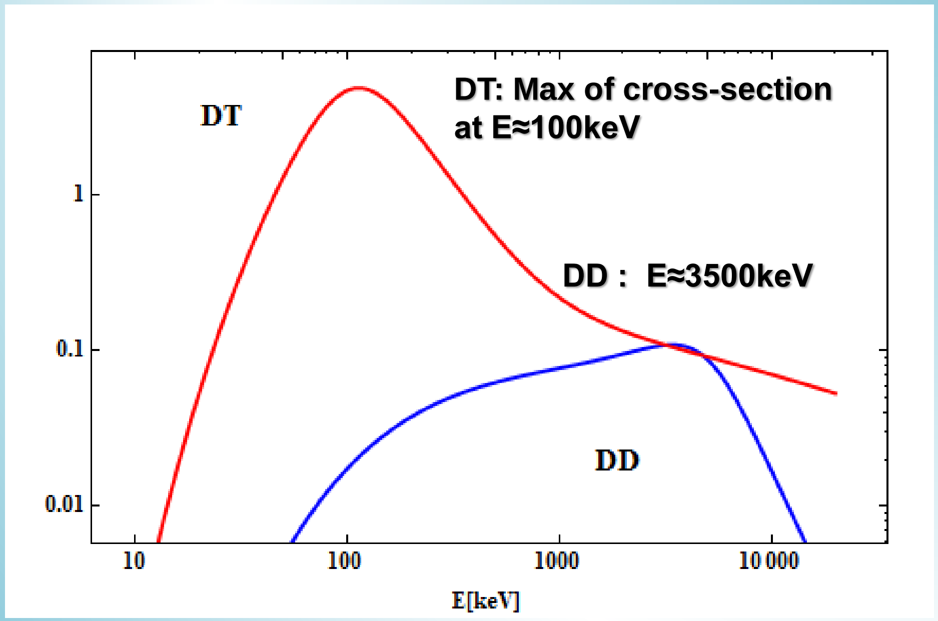

Stopping length of Deutrons in Titanium (experimental data)

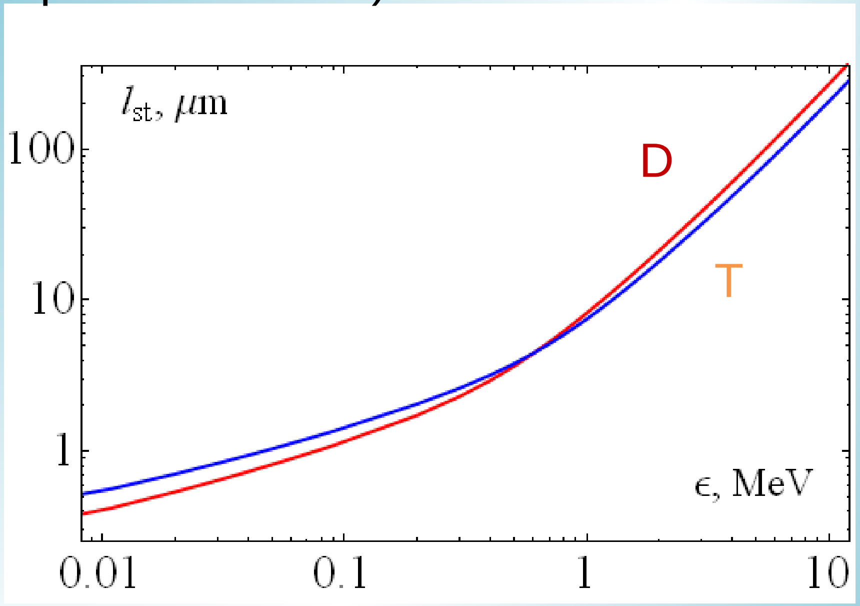

Результаты оптимизации для E_L= 5 мДж

№	тип мишень/лазер	средняя плотность, n_{av}/n_0	высота, h/λ_L.	диаметр, d/λ_L	абсолютный выход DD	выход DD на 1 Дж
1	проволоки/I	0,07	1,5	0,3	5×10^3	10^6
2	проволоки/I	0,13	1,5	0,4	5×10^3	10^6
3	проволоки/II	0,28	3	0,6	10^4	2×10^6
4	проволоки/II	0,04	7,5	0,4	5×10^3	10^6
5	слои/I,p	0,2	3	0,2	4×10^3	8×10^5
6	слои/I,p	0,4	3	0,4	2×10^3	4×10^5
7	слои/I,s	0,4	3	0,4	5×10^2	10^5

N_D~3*10^{10}

Выход нейтронов (микро-цилиндры)

$$N = V\sigma_0 v_D t_r n_a n_D,\ \ t_r \simeq l_{st}^D / v_D$$

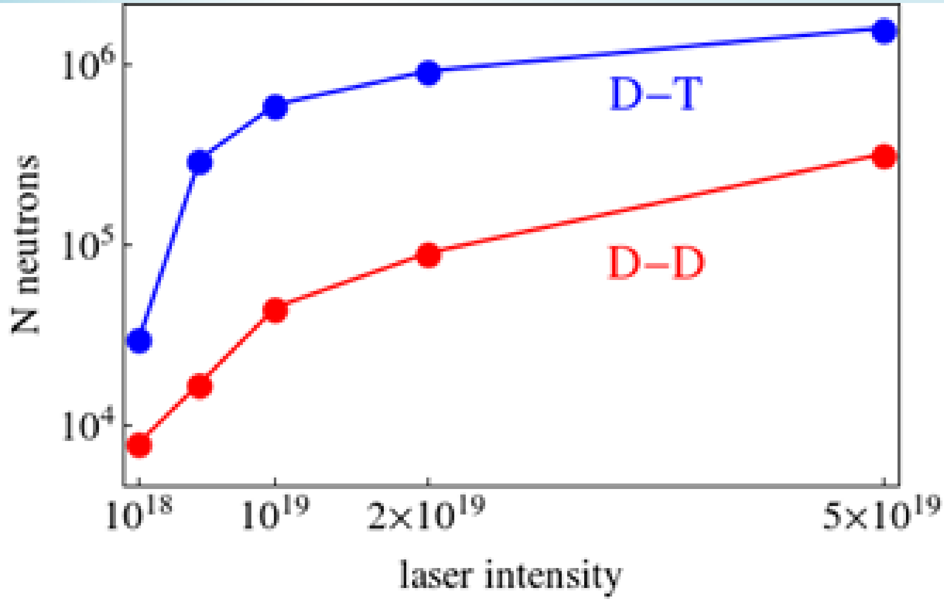

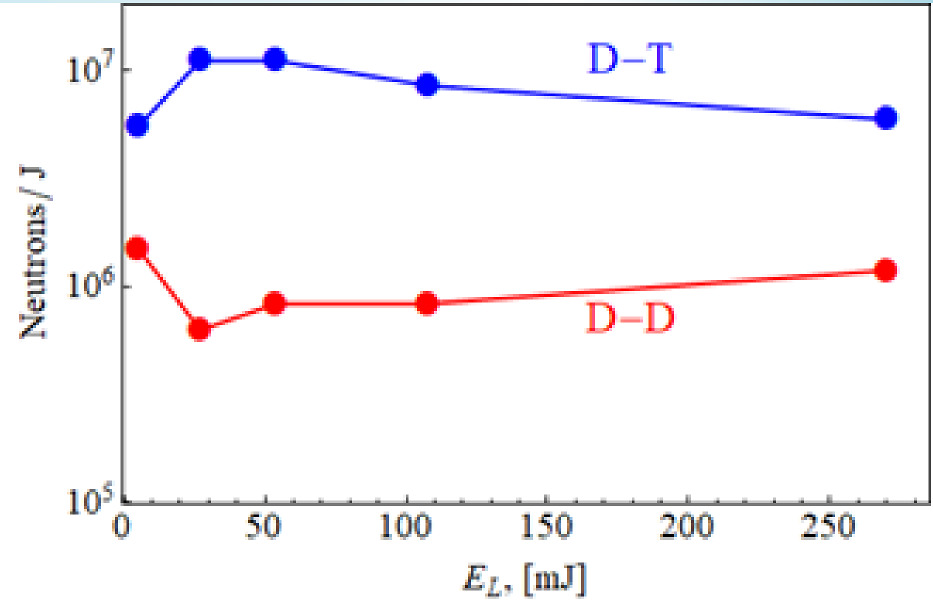

D_L = 4 λ_L (FMHW), τ =30 **fs**

N_D~3*10^{10} (E_d>50keV, I_L ≈10^{18} Wcm^{-2}), dN_D/N_{D0} ≈30-60 %

Neutron yield (25 mJ, 0.1 kHz)

5*10^7 neutrons/s (DD) and 10^9 neutrons/s (DT)

Выводы

- Объемный стохастический нагрев микро-структрированной мишени, генерация супер-пондеромотоных электронов
- Эффективное ускорение дейтронов, повышение эффективности термоядерных реакций
- Выход нейтронов для лазера 25мДж, 1кГц $5 \cdot 10^{7}$ (DD) и $\cdot 10^{9}$ (DT) нейтронов/сек
- Применение микро-слоев более перспективно, тк технологических слои легче произвести

Спасибо за внимание!!

D.A. Gozhev, S.G. Bochkarev, N.I. Busleev., A.V. Brantov, S.I. Kudryashov, A.B. Savel'ev, V.Yu, Bychenkov High Energy Density Phys. **37**, 75 (2020).

S.G. Bochkarev, A.V. Brantov, D. A. Gozhev Journal of Russian Laser Research **42**, (2021), in press.

Nano-scaled targets application in laser plasma experiments

S. Jiang et al., PRL **116** 085002 (2016)
A.Lubcke et al., SRep **7**, 44030 (2017)
C. Bargsten et al., SAdv **3**, e1601558 (2017)
J.J. Rocca et al., Laser Focus World, May 2017
A. Curtis et al., Nature Comm. **9** 1177 (2018)
M.A. Purvis, Nature Photon., **7** 796 (2013)

SEM image Silicon wires

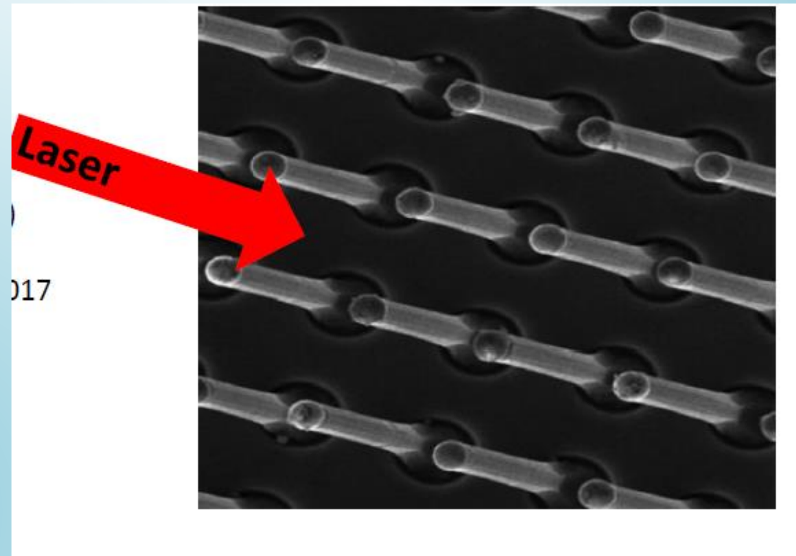

SEM image deteurated carbon nanowires, CD2

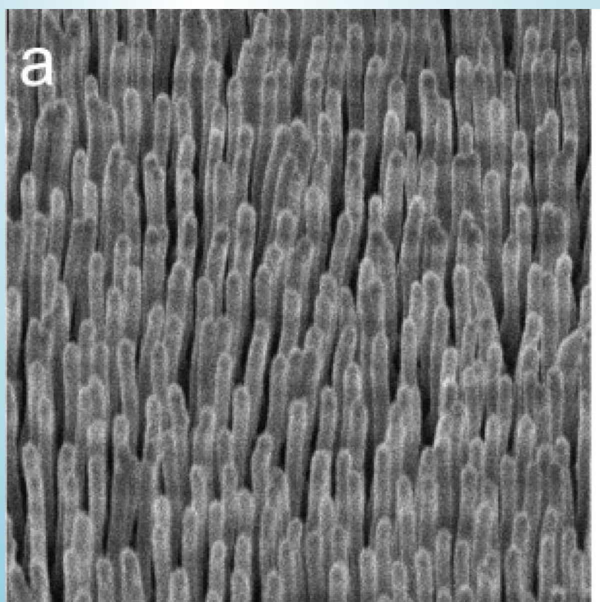

SEM images Ni-Co wires

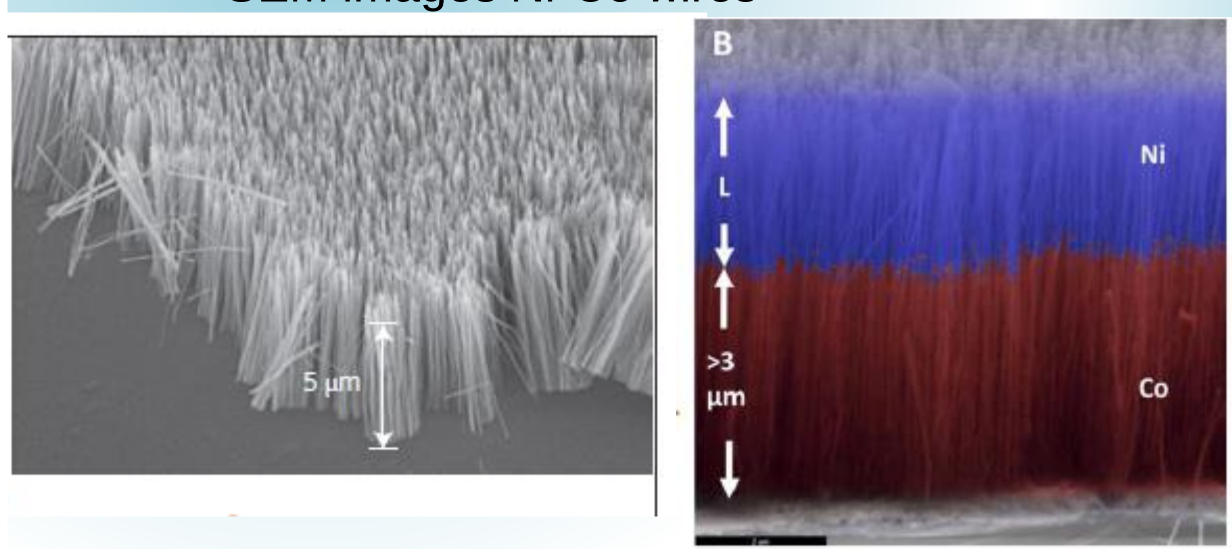

Electron heating

EM field penetration (volume heating)

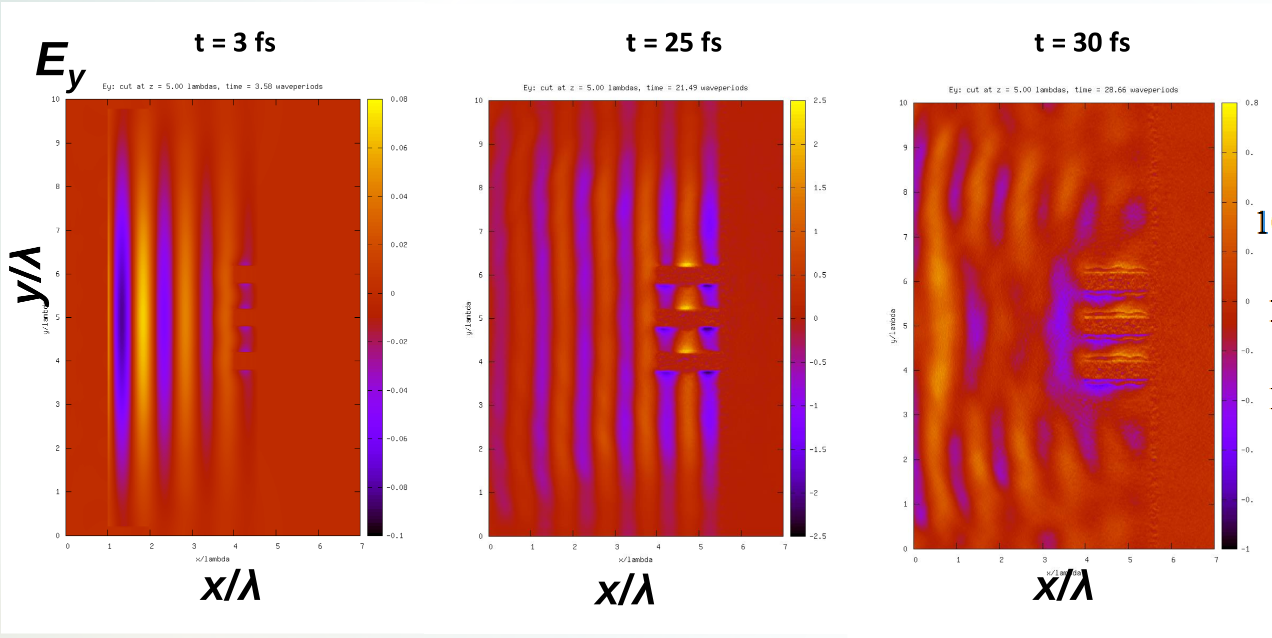

Electron energy spectra

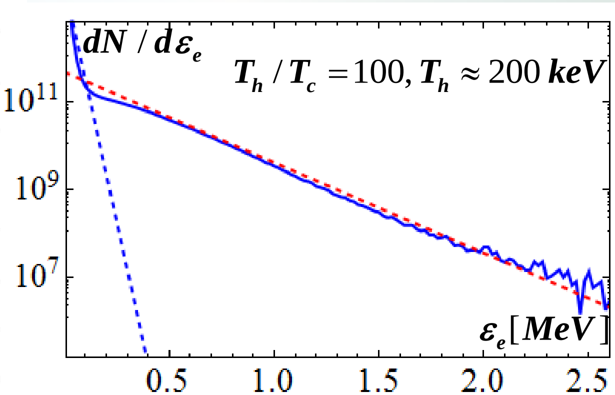

Phase space distribution (x,p_x)

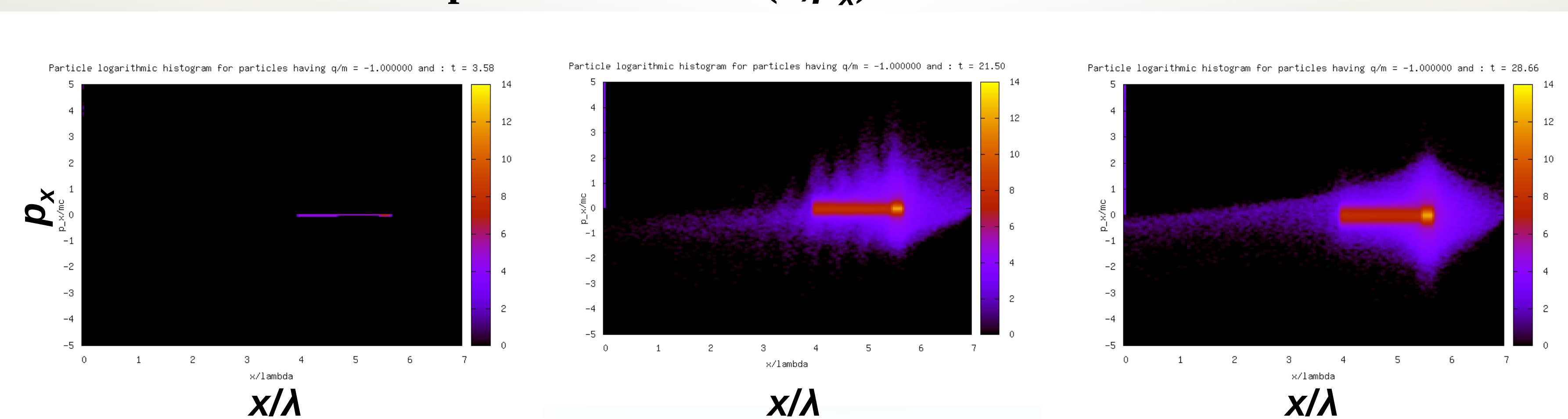

Energy spectra and plasma expansion

Time evolution of energy spectrum

Evolution of cut-off energy energy

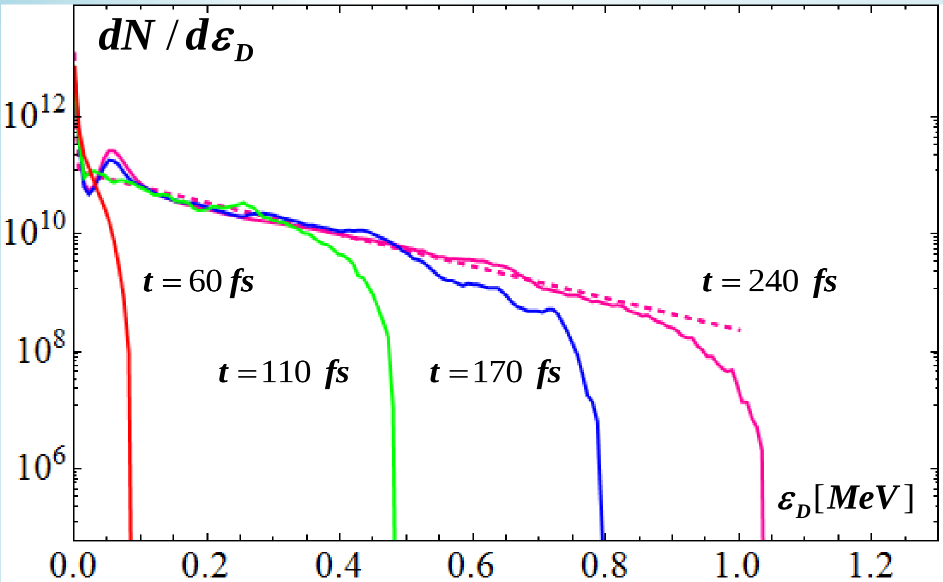

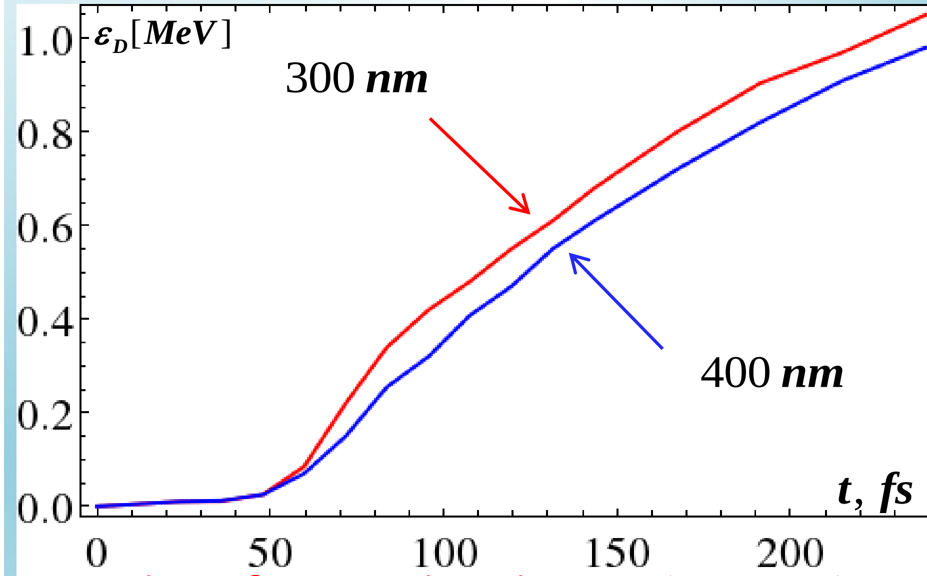

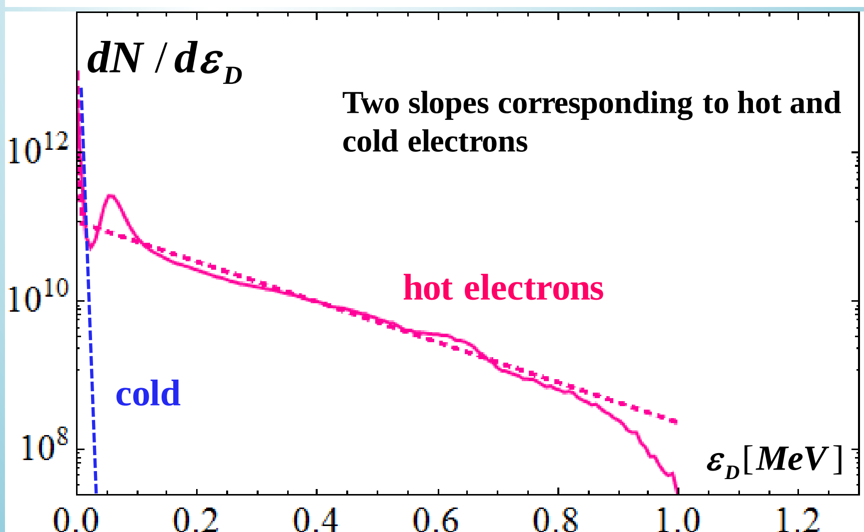

Conversion of energy into ions 6 (400 nm) 10 % (300 nm)

Approximation for spectrum

$$\frac{dN}{d\varepsilon_2} = \theta(\varepsilon_{ch}-\varepsilon_2)Cn_{c0}\exp\left(\frac{-\varepsilon_2}{Z_2T_c}\right)+\theta(\varepsilon_2-\varepsilon_{ch})Cn_{h0}\exp\left(\frac{-\varepsilon_2}{Z_2T_h}\right),$$

$$\varepsilon_{ch} = Z_2T_c\ln(n_{c0}/n_{h0}),$$

V.F.Kovalev, S.G.Bochkarev and V.Yu.Bychenkov, V.T. Tikhonchuk, *Quantum Electron.*, **47**, 1023 (2017).

Results of optimization for a 5 mJ laser pulse

run	Target/ Laser	d/λ_L	h/λ_L	n_{av}/n_0	Y_{DD}	Y_{DT}	N_{DD}, neutrons/J	N_{DT} neutrons/J
1	wires/ set I	0.3	1.5	0.07	3×10^{-8}	1×10^{-6}	2×10^{5}	1×10^{7}
2	wires/ set I	0.4	1.5	0.13	1×10^{-8}	7×10^{-7}	2×10^{5}	1×10^{7}
3	wires/II	0.6	3	0.28	1×10^{-8}	5×10^{-7}	4×10^{5}	2×10^{7}
4	wires/II	0.4	7.5	0.04	9×10^{-9}	6×10^{-7}	3×10^{5}	2×10^{7}
5	sheets/I, p-polar.	0.2	3	0.2	1×10^{-9}	2×10^{-7}	7×10^{4}	8×10^{6}
6	sheets/I, p-polar.	0.4	3	0.4	4×10^{-10}	5×10^{-8}	4×10^{4}	5×10^{6}
7	sheets/I, s-polar.	0.4	3	0.4	10^{-10}	1×10^{-8}	10^{4}	2×10^{6}

set I

$I_L=10^{18}$ W/cm^2,
$D_L = 4\lambda_L$
$\tau = 30$ fs

set II

$I_L=2\cdot10^{18}$ W/cm^2,
$D_L = 2\lambda_L$
$\tau = 60$ fs

Stochastic electron heating

Laser pulse field and arbitrary additional field (E.M. fields, electrostatic field, Coulomb, quasistatic magnetic field)

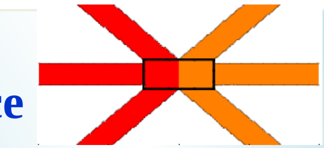

Colliding laser pulses, incident and reflected waves in preplasma

inc. and reflected (scattered) light at sharp plasma-vacuum interface

Z.M. Sheng et al. PRE **69**, 016407 (2004)

Y. Sentoku V.Yu. Bychenkov et al., Appl. Phys. B**74** 207 (2002)

Rax, Phys

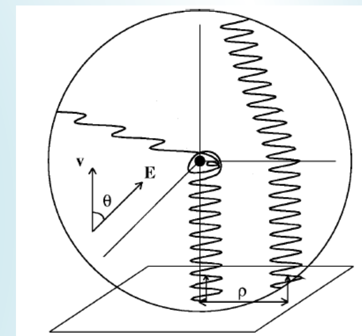

Interaction of laser pulse with Coulomb field (e-i collisions in a strong E.M. field, interaction with nano/micro targets)

A. Brantov,W Rozmus et al., Phys Plasmas 10 3385 (2003).

Electromagnetic field and quasi-static magnetic field

A. Bourdier et al. Physica D: Nonlinear Phenom**. 206** 1 (2005).

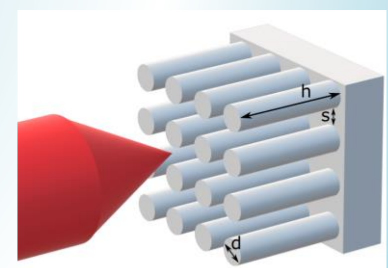

SMWFA (wake field from a pulse front)

N.E. Andreev et al., Las. Part. Beams 34 115 (2016)

How to determine stochastic behavior?

Lyapunov exponents: A.J. Lichtenberg, M.A. Lieberman Regular and Chaotic Dynamics, 2nd ed., Applied Mathematical Sciences, Vol. 38, New York

Outline

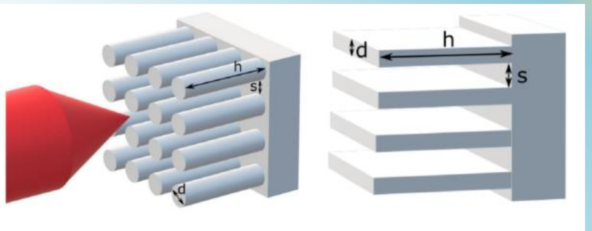

- PIC simulation of volumetric heating and optimization of target characteristics for innovative high-average-density **structured micro-wires/sheets** targets irradiated by moderately intense pulses ($I_L \geq 10^{18}$ W/cm^2, $\lambda_L = 0.8\text{-}1\ \mu m$), this is the first candidate for generating pulses with a high repetition rate
- Mechanisms of electron heating (DLA/vacuum heating and stochastic acceleration), **generation of supra- ponderomotive particles**, rigorous analysis: stochastic electron dynamics (the largest Lyapunov exponent) and test particle method
- The **deuterons/tritium acceleration** from such high-average density targets, neutron sources from DD and DT reactions

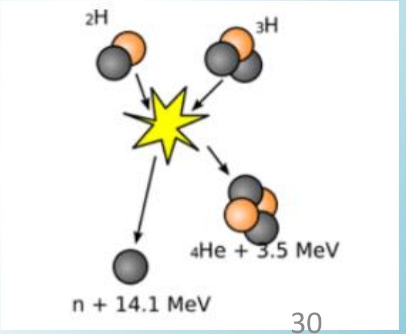

- Conclusions

Анализ устойчивости траекторий

- **Autocorrelation Function**

$$A(\tau) = \lim_{T\to\infty} \frac{1}{T}\int_0^T X(t)X(t+\tau)\,dt$$

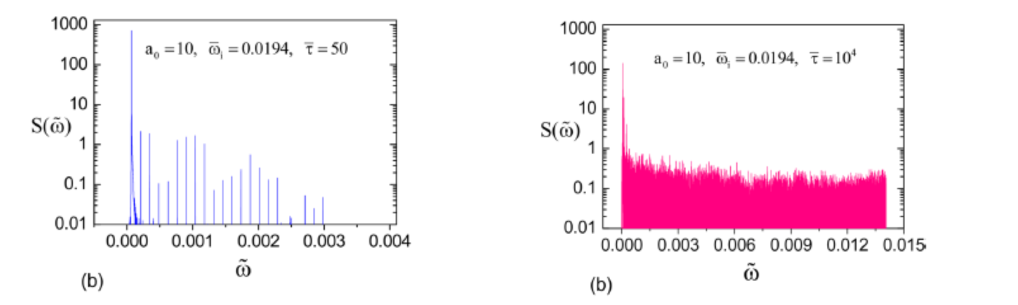

Stochastic trajectories: **transition** from a **discrete** to a **continuous spectrum**

PHYSICS OF PLASMAS 17, 093103 (2010)

- **Spectral Analysis**

$$X(\omega) = \int_0^{T_0} X(t)\exp(-i\omega t)\,dt$$

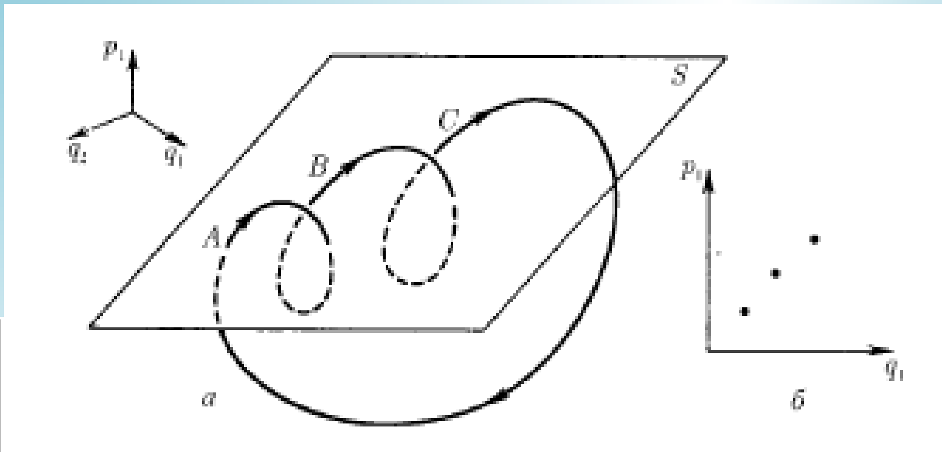

- **Poincaré section**

regular

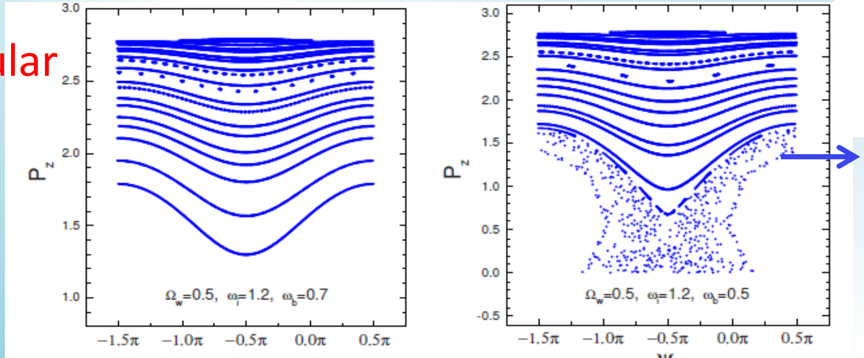

chaotic

Stochastic electron heating

Laser pulse field + arbitrary additional field (e.m. field, electrostatic field, coulomb, magnetic field)

Colliding laser pulses [Rax, Z.M. Sheng et al. PRE 69, 016407 (2004), Y. Sentoku Appl. Phys. B74 207 (2002)]

V.S. Rastunkov and V.P. Krainov Laser Phys. 15 262 (2005)]

Interaction of laser pulse with Coulomb field (e-i collisions in a strong e.m. field, interaction with nano/micro targets)

Electromagnetic field and quasi-static magnetic field

Laser pulse and plasma wave (wake field from a pulse front)

For micro wire array target:

G. Cristoforetti et al., Scientific Reports, **7** 1479 (2017).

D.A. Serebryakov et al., Plasma Phys. Control. Fusion **61** 074007 (2019).

regular chaotic

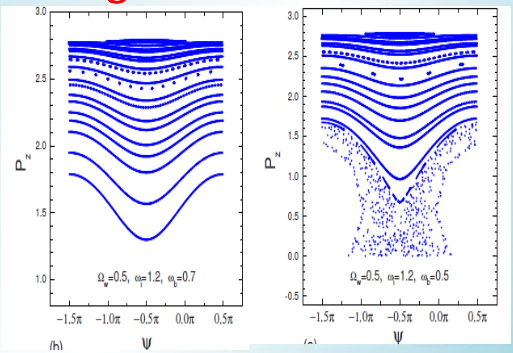

Описание квазистатических поле в микро структурах

$$E_y^i = E_0 f(r)\cos(\phi_-),\quad E_y^r = \hat{r}E_0 f(r)\cos(\phi_+ + \pi),\quad B_z^i = E_0 f(r)\cos(\phi_-),\quad B_z^r = \hat{r}E_0 f(r)\cos(\phi_+),$$

$$\phi_\pm = \omega_L t \pm k_L x + \phi_0,\ f(r) = \sum_{n=1}^{N_{str}} \exp\left(-\frac{(d/2-|\vec{R}_n|)}{l}\right).$$

$$\vec{\mathbf{E}}^C(\vec{\mathbf{r}}) = E_{Q0}\frac{m_e c\omega_L}{e}\sum_{n=1}^{N_{str}}\begin{cases} 0, \\ \left(1-\frac{d}{2l_s}+\frac{|\vec{\mathbf{R}}_n|}{l_s}\right)\frac{\vec{\mathbf{R}}_n}{|\vec{\mathbf{R}}_n|}, \\ \frac{C_Q\vec{\mathbf{R}}_n}{|\vec{\mathbf{R}}_n|^2}\exp\left(\frac{-|\vec{\mathbf{R}}_n|}{r_d}\right), \end{cases}$$

$$\vec{\mathbf{R}}_n = \vec{\mathbf{r}}_\perp - \vec{\mathbf{r}}_n,\quad C_Q = \frac{d}{2}\exp\left(\frac{d}{2r_d}\right),$$

$$j_\parallel(r = |\vec{\mathbf{R}}_n|) = -ecn_{\mathbf{cr}}B_{\phi 0}\begin{cases} 0, & r \le d/2 - l_s \\ C_{j1}(r-d/2+l_s)(r-d/2), & d/2-l_s < r \le d/2 \\ C_{j2}\exp\left(-\frac{r}{r_{\mathbf{E}}}\right)(r-d/2), & r > d/2. \end{cases}$$

$$B_\phi^0(r_\perp) = \frac{4\pi}{cr_\perp}\int_0^{r_\perp} j_\parallel(r)\,r\,dr.$$

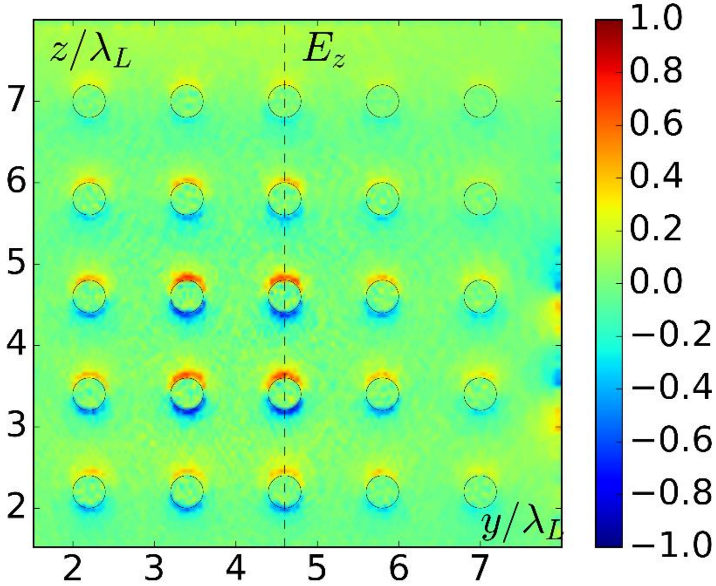

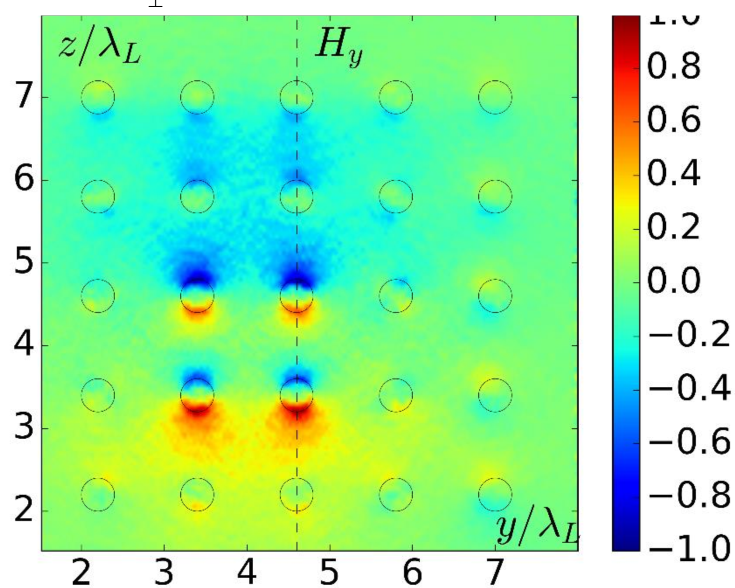

$$\hat{r} \approx 0.7$$

$$E_{Q0}/E_0 \approx 0.7$$

$$B_{\phi 0}/E_0 \approx 0.6$$